UNIVERSITY
OF
SOUTHAMPTON

DEPARTMENT OF SHIP SCIENCE

FACULTY OF ENGINEERING

AND APPLIED SCIENCE

# PREDICTION OF THE MANOEUVRING FORCES ON A SLENDER SHIP USING SLENDER BODY THEORY PART IV: PLANAR MOTION EXPERIMENTS AND SLENDER BODY CALCULATIONS APPLIED TO A LEANDER CLASS FRIGATE MODEL

J. Cross-Whiter, J.F. Wellicome, P.A. Wilson, X. Cheng

Ship Science Report 81
April 1994

Final Report on the Project

# Prediction of the Manoeuvring Forces on a Slender Ship Using Slender Body Theory

## Part IV

## Planar Motion Experiments and Slender Body Calculations Applied to a Leander Class Frigate Model

by

J. Cross-Whiter, J. F. Wellicome, P. A. Wilson

and

X. Cheng

Department of Ship Science
University of Southampton

April 1994

## INTRODUCTION

A series of tests were conducted on a 1:45 model of a Leander class frigate in February, 1994, using the Planar Motion Mechanism (PMM) at the Southampton Institute of Higher Education. This facility and equipment are described in References [1], [2]. The model particulars are given in Table 1. The model comprised a naked hull with no rudders or other appendages.

Table 1. Base Leander Model Particulars

| | |
|---|---|
| Scale | 1:45 |
| LWL | 2440 mm |
| Beam | 273 mm |
| Draught | 94 mm |
| Displacement | 31.3 kg |
| LCG | 76 mm abaft amidships |

This model configuration was tested at three forward speeds and two frequencies. In addition a reduced set of tests was run with the LCG shifted forward to 55 mm abaft amidships.

## MODEL PREPARATION

Prior to testing the model was ballasted to give the specified displacement and LCG. Its dry yaw radius of gyration was also determined, but not adjusted to a specified value, since the results can be numerically corrected to any radius of gyration. The radius of gyration was determined by suspending the model from two thin lines, 3.715 m long, attached 0.860 m forward and aft of amidships. The model was swung in a pure yaw motion and the radius of gyration determined from :

$$K = \frac{TD}{4\pi}\sqrt{G/L}$$

where:

K = yaw radius of gyration
T = swing period
D = pendulum attachment point separation
G = gravitation acceleration
L = pendulum length

The measured radius of gyration was 0.463 m.

The model was not fitted with turbulence stimulators, as previous tests had indicated negligible effect on the motion coefficients (see Reference [2]).

The PMM dynamometry was calibrated on a bench at the towing tank and installed in the model, with the centre of the baseplate at the base model LCG.

## TEST PROCEDURE

Tests were conducted in static mode, in which the model is held at a fixed angle of attack to the carriage motion; pure sway mode, in which the two PMM struts are moved transversely in phase; and pure yaw

mode, in which the struts are moved at different phases giving a pure yaw motion relative to the model direction of travel. Strut motion and dynamometer force data were collected during each run and stored on computer discs for later analysis.

Static tests were conducted at 1.23, 1.50 and 1.84 m/s speeds, at drift angles of -6 to +12 degrees, in steps of 2 degrees.

With the LCG at its original (76 mm) position pure sway and pure yaw tests were conducted at speeds of 1.23, 1.50 and 1.84 m/s and strut oscillation periods of 4.8 and 6.4 seconds. For each combination of speed and period tests were conducted for a series of strut transverse amplitudes to give yaw angles of 2, 4, 6, 8 and in some cases, 10 and 12 degrees.

With the LCG at its forward (55 mm) position pure sway and yaw tests were conducted at speeds of 1.50 and 1.84 m/s and periods of 6.4 seconds.

## TEST RESULTS

The test results are presented in Tables 2 through 7 and Figures 1 through 28. In these tables and figures the following terms are used:

$Y_v'$, $Y_{vvv}'$, $N_v'$, $N_{vvv}'$ = Non-dimensional first and third derivatives of sideforce and yaw moment with respect to transverse velocity, as conventionally defined (see, for example Reference [3]).

$Y_{\dot{v}}'$, $N_{\dot{v}}'$ = Non-dimensional first derivatives of sideforce and yaw moment with respect to transverse acceleration, as conventionally defined.

$Y_r'$, $Y_{rrr}'$, $N_r'$, $N_{rrr}'$ = Non-dimensional first and third derivatives of sideforce and yaw moment with respect to yaw rate, as conventionally defined.

$Y_{\dot{r}}'$, $N_{\dot{r}}'$ = Non-dimensional first derivatives of sideforce and yaw moment with respect to yaw acceleration, as conventionally defined.

$m'$ = Non-dimensional mass = $m/(1/2\rho L^3)$

$x_{G,m}'$ = Non-dimensional distance from baseplate centre to LCG, midships = $x_{G,m}/L$. Note that $x_G$ is zero for the base condition, since the baseplate was centred at the original LCG.

$I_z'$ = Non-dimensional dry yaw moment of inertia

$N_u$ = $m'x_G'u_0(1 + \alpha^2/8)$, where $u_0$ = towing speed/total speed, $\alpha^2 = (a\omega\cos\epsilon)^2/u_0^2$, a = dynamometer strut transverse amplitude, $\omega$ = strut frequency, $\epsilon = \sin^{-1}(\omega x_s/u_0)$, $x_s$ = 1/2 strut separation/L

$Y'$, $N'$ = Non-dimensional sideforce, yaw moment

$v'$ = Transverse velocity/total velocity

Y1in, N1in = Linear in-phase components in Fourier series representation of sideforces and moments

Y1quad, N1quad = Linear quadrature components in Fourier series representation of sideforces and moments

The mathematics and nomenclature used in the analysis of the PMM results are discussed in more detail in References [1] and [2].

The yaw moment coefficients given herein are all defined relative to the baseplate centre. To derive the moment coefficients about the midships point the following equations are used:

$$N_{vm}' = N_v' - Y_v'x_m'$$
$$N_{vvvm}' = N_{vvv}' - Y_{vvv}'x_m'$$
$$N_{\dot{v}m}' = N_{\dot{v}}' - Y_{\dot{v}}'x_m'$$
$$N_{rm}' = N_r' - Y_r'x_m'$$
$$N_{rrrm}' = N_{rrr}' - Y_{rrr}'x_m'$$
$$N_{\dot{r}m}' = N_{\dot{r}}' - Y_{\dot{r}}'x_m'$$

The additional subscript m refers to the midship position.

The sideforce and yaw moment coefficients derived from the static tests at the original LCG are given in Table 2, and the curves which were fitted to yield these results are shown in Figures 1 and 2. The coefficients for the static tests with the LCG at the forward position are given in Table 5, and the corresponding curves are shown in Figures 3 and 4. The coefficients from the sway tests at the original LCG are given in Table 3 and the corresponding curves are shown in Figures 5 through 16. Figures 9 through 16 also include the results of the tests with the LCG at the forward position. The coefficients derived from the forward LCG curves are given in Table 6. The coefficients from the yaw tests at the original LCG are given in Table 4, and the corresponding curves are shown in Figures 17 through 28. Figures 21 through 28 also include the results of the tests at the forward LCG position, and the coefficients derived from these curves are given in Table 7.

Table 2. Static Test Force Coefficients - Original LCG

| Speed | $Y_v'$ | $1/6Y_{vvv}'$ | $N_v'$ | $1/6N_{vvv}'$ |
|---|---|---|---|---|
| 1.23 | -0.00737 | -0.18509 | -0.00404 | -0.05683 |
| 1.50 | -0.00691 | -0.21921 | -0.00401 | -0.06827 |
| 1.84 | -0.00762 | -0.14187 | -0.00452 | -0.05172 |

Table 3. Sway Test Force Coefficients - Original LCG

| Speed (m/s) | Period (sec) | $Y_v'$ | $1/6Y_{vvv}'$ | $N_v'$ | $1/6N_{vvv}'$ | $m'-Y_{\dot{v}}'$ ($x10^3$) | $mx_G-N_{\dot{v}}'$ ($x10^4$) |
|---|---|---|---|---|---|---|---|
| 1.23 | 4.8 | -0.00561 | -0.14028 | -0.00421 | -0.03496 | -7.69014 | -2.65715 |
| 1.23 | 6.4 | -0.00553 | -0.14153 | -0.00401 | -0.03622 | -7.46577 | -2.97690 |
| 1.50 | 4.8 | -0.00609 | -0.13020 | -0.00451 | -0.03675 | -7.87258 | -1.73670 |
| 1.50 | 6.4 | -0.00617 | -0.14163 | -0.00435 | -0.03922 | -7.60647 | -3.01811 |
| 1.84 | 4.8 | -0.00740 | -0.14685 | -0.00480 | -0.02459 | -8.39836 | -1.16575 |
| 1.84 | 6.4 | -0.00648 | -0.18748 | -0.00453 | -0.04253 | -8.44465 | -2.88818 |

Table 4. Yaw Test Force Coefficients - Original LCG

| Speed (m/s) | Period (sec) | $Y_r'$ | $1/6Y_{rrr}'$ | $N_r'-N_u$ | $1/6N_{rrr}'$ | $m'-Y_{\dot{r}}'$ ($x10^4$) | $I_z'-N_{\dot{r}}'$ ($x10^4$) |
|---|---|---|---|---|---|---|---|
| 1.23 | 4.8 | -0.00464 | -0.00459 | -0.00133 | -0.00301 | 4.26398 | 3.80559 |
| 1.23 | 6.4 | -0.00414 | -0.00937 | -0.00121 | -0.00455 | 5.67091 | 3.82180 |
| 1.50 | 4.8 | -0.00435 | -0.00753 | -0.00136 | -0.00475 | 5.62797 | 3.84499 |
| 1.50 | 6.4 | -0.00432 | -0.00960 | -0.00136 | -0.00481 | 6.17376 | 4.32006 |
| 1.84 | 4.8 | -0.00473 | -0.00116 | -0.00171 | -0.00398 | 8.12418 | 4.24324 |
| 1.84 | 6.4 | -0.00434 | -0.01047 | -0.00161 | -0.00615 | 7.89252 | 4.85440 |

Table 5. Static Test Force Coefficients - Forward LCG

| Speed | $Y_v'$ | $1/6Y_{vvv}'$ | $N_v'$ | $1/6N_{vvv}'$ |
|---|---|---|---|---|
| 1.23 | -0.00760 | -0.18835 | -0.00429 | -0.05847 |
| 1.50 | -0.00647 | -0.32760 | -0.00428 | -0.08587 |
| 1.84 | -0.00717 | -0.35551 | -0.00519 | -0.04595 |

Table 6. Sway Test Force Coefficients - Forward LCG

| Speed (m/s) | Period (sec) | $Y_v'$ | $1/6Y_{vvv}'$ | $N_v'$ | $1/6N_{vvv}'$ | $m'-Y_{\dot{v}}'$ ($x10^3$) | $mx_G'-N_{\dot{v}}'$ ($x10^4$) |
|---|---|---|---|---|---|---|---|
| 1.50 | 6.4 | -0.00564 | -0.21179 | -0.00451 | -0.05340 | -7.81241 | -4.74684 |
| 1.84 | 6.4 | -0.00673 | -0.22891 | -0.00496 | -0.05138 | -8.48275 | -3.54397 |

Table 7. Yaw Test Force Coefficients - Forward LCG

| Speed (m/s) | Period (sec) | $Y_r'$ | $1/6Y_{rrr}'$ | $N_r'-N_u$ | $1/6N_{rrr}'$ | $m'-Y_{\dot{r}}'$ ($x10^4$) | $I_z'-N_{\dot{r}}'$ ($x10^4$) |
|---|---|---|---|---|---|---|---|
| 1.50 | 6.4 | -0.00447 | -0.01180 | -0.00152 | -0.00537 | 7.36552 | 4.31220 |
| 1.84 | 6.4 | -0.00456 | -0.01390 | -0.00175 | -0.00722 | 8.46825 | 4.70095 |

## NUMERICAL CALCULATIONS

A computation code based on the slender body theory (Ref.[4]) was applied to the Leander hullform to calculate the sway force and yaw moment, and the calculated results were compared with the measured data from the present PMM tests.

The Leander hullform is shown in Fig.29 which was reproduced by digitizing an original body plan provided by Haslar. The original body plan contained 25 sections from which 38 evenly divided sections were produced by interpolation. These 38 sections were used in the calculation.

Fig.30 and Fig.31 show the calculated streamlines on the hull at zero drift angle. The calculated sway force and yaw moment were given in Fig.32 and Fig.33 in comparison with the PMM measurement. It can be seen that calculation under estimated the sway force and over estimated the yaw moment, which is consistent with the calculations carried out for the Mariner hull and British Bombardier hull using the same code. However in this case the agreement between the calculation and the PMM tests is quite satisfactory for both sway force and yaw moment, in contrast to other cases in which poor agreement was found for the yaw moment. Since the slender body theory is based on certain assumptions on the hullform, it is not unexpected to see the different accuracies when the theory is applied to different hullforms. Fig.34 shows the calculated side force distribution on the Leander hull. Some irregularities are found near the stern, which might be caused by the steep change of the hull section geometry in that area as can be seen in Fig.30.

## CONCLUSIONS

In general the results display consistent behaviour with respect to changes in oscillation period and forward speed. As has been found in previous tests (see References [1], [2]) the third derivative terms often exhibit wide scatter, but the manoeuvring characteristics of the vessel are determined principally by the lower order terms. As the sway period is increased the linear sideforce coefficients ( $Y_v'$) from the sway tests do not appear to converge to the values obtained from the static tests, whereas the yaw moment coefficients ($N_v'$) do.

The oscillation periods are restricted by the run length available in the towing tank. The periods for this series of tests were chosen to allow two full oscillation cycles during the run, at all speeds. Longer periods are needed to resolve the extrapolation of results to zero frequency. Tests could be conducted at longer periods, taking data during only one oscillation cycle. Alternatively, the PMM rig could be taken to a longer towing tank, enabling longer run time.

The centre of pressure for the original LCG, derived by dividing the static $N_v'$ by $Y_v'$, ranges from 0.584L to 0.593L, i.e. is forward of the stem. For the forward LCG position, it is further forward, ranging from 0.564L to 0.724L. The sideforce coefficients from the yaw tests ($Y_r'$) appear high relative to the yaw moment coefficients ($N_r'$). This is consistent with the forward position of the centre of pressure derived from the static tests.

The calculation results show that the sideforce and yaw moment are lower and higher, respectively, than the measured data, but the agreement is generally good.

## REFERENCES


[1] Wellicome, J. F., Wilson, P. A. and Cheng, X. 1994
*Prediction of the Manoeuvring Forces on a Slender Ship Using Slender Body Theory Part II: Towing Tank Tests Using Planar Motion Mechanism*
Ship Science Report No.74, University of Southampton

[2] Wilson, P. A., Wellicome, J. F. and Cheng, X. 1993
*Progress Report No. 6 to MOSES Participants Meeting*

[3] Mandel, P. 1967
*Ship Manoeuvring and Control* in <<Principles of Naval Architecture>>
John P. Comstock, ed., The Society of Naval Architects and Marine Engineers, New York, 1967

[4] Wellicome, J. F., Wilson, P. A. and Cheng, X. 1994
*Prediction of the Manoeuvring Forces on a Slender Ship Using Slender Body Theory Part I: Theoretical Estimates of Forces* and *Moments*
Ship Science Report No.73, University of Southampton

Fig.1 Leander Static Test Y′ vs v′

Original LCG

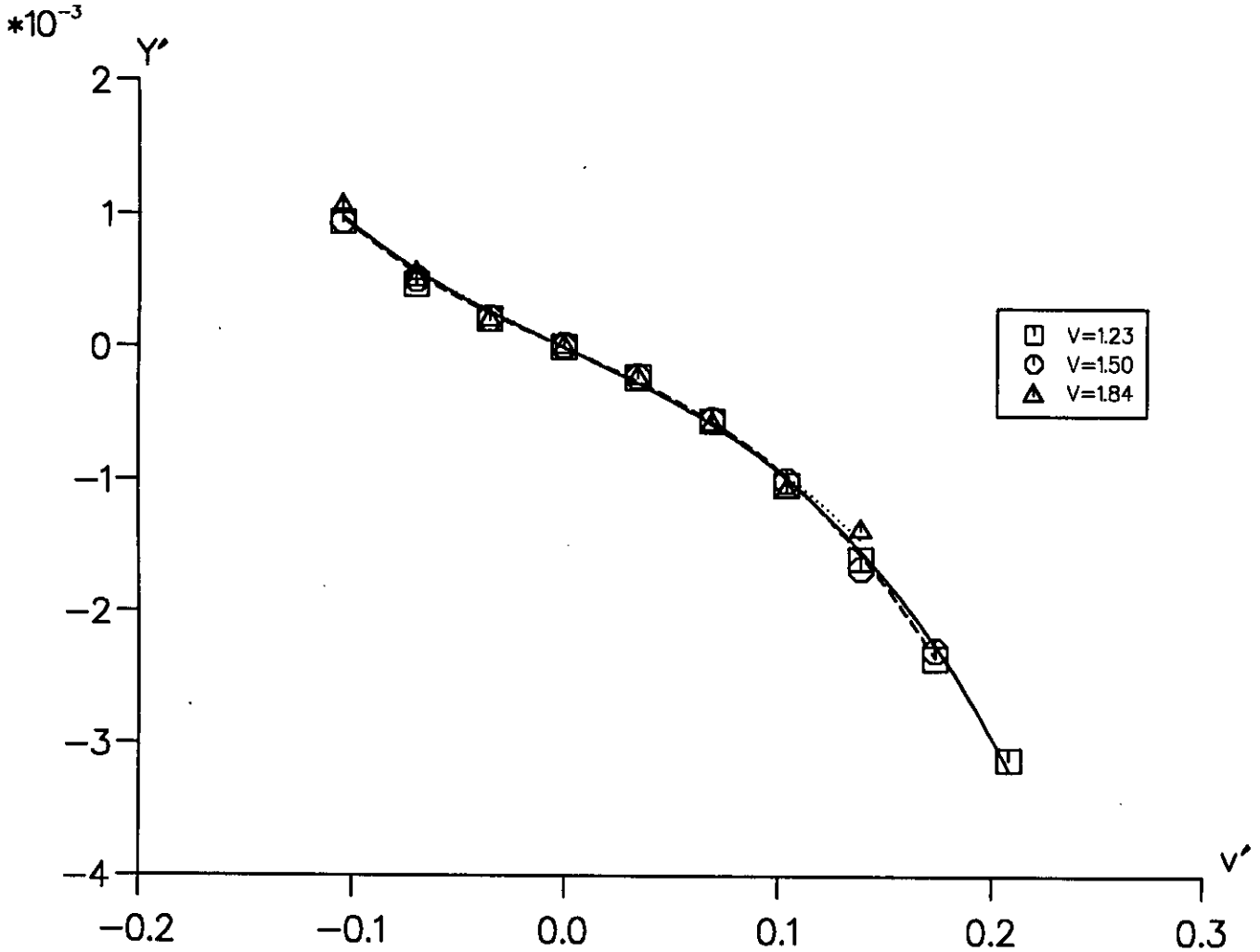

Fig.2 Leander Static Test N′ vs. v′

Original LCG

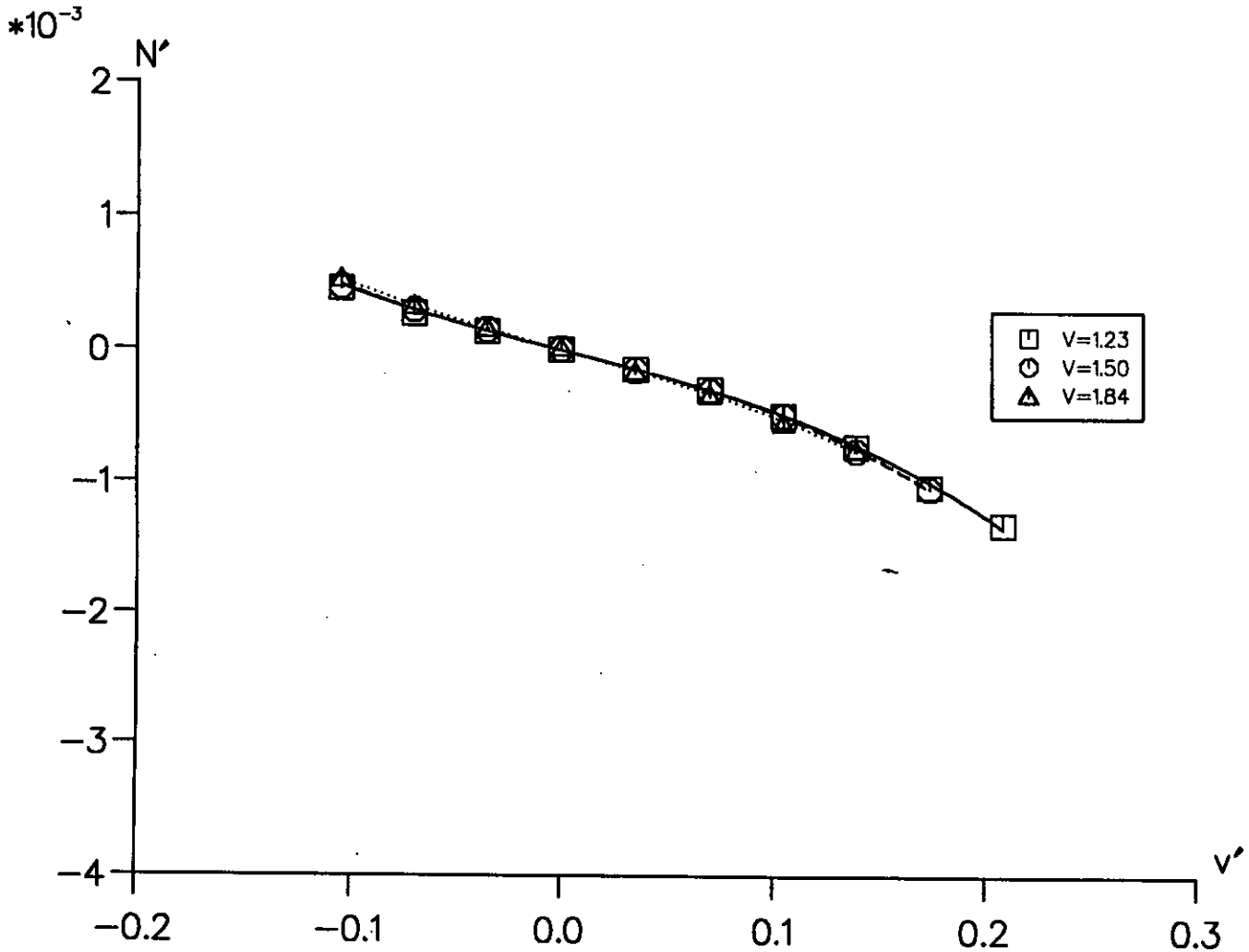

Fig.3 Leander Static Test Y′ vs. v′

Fwd LCG

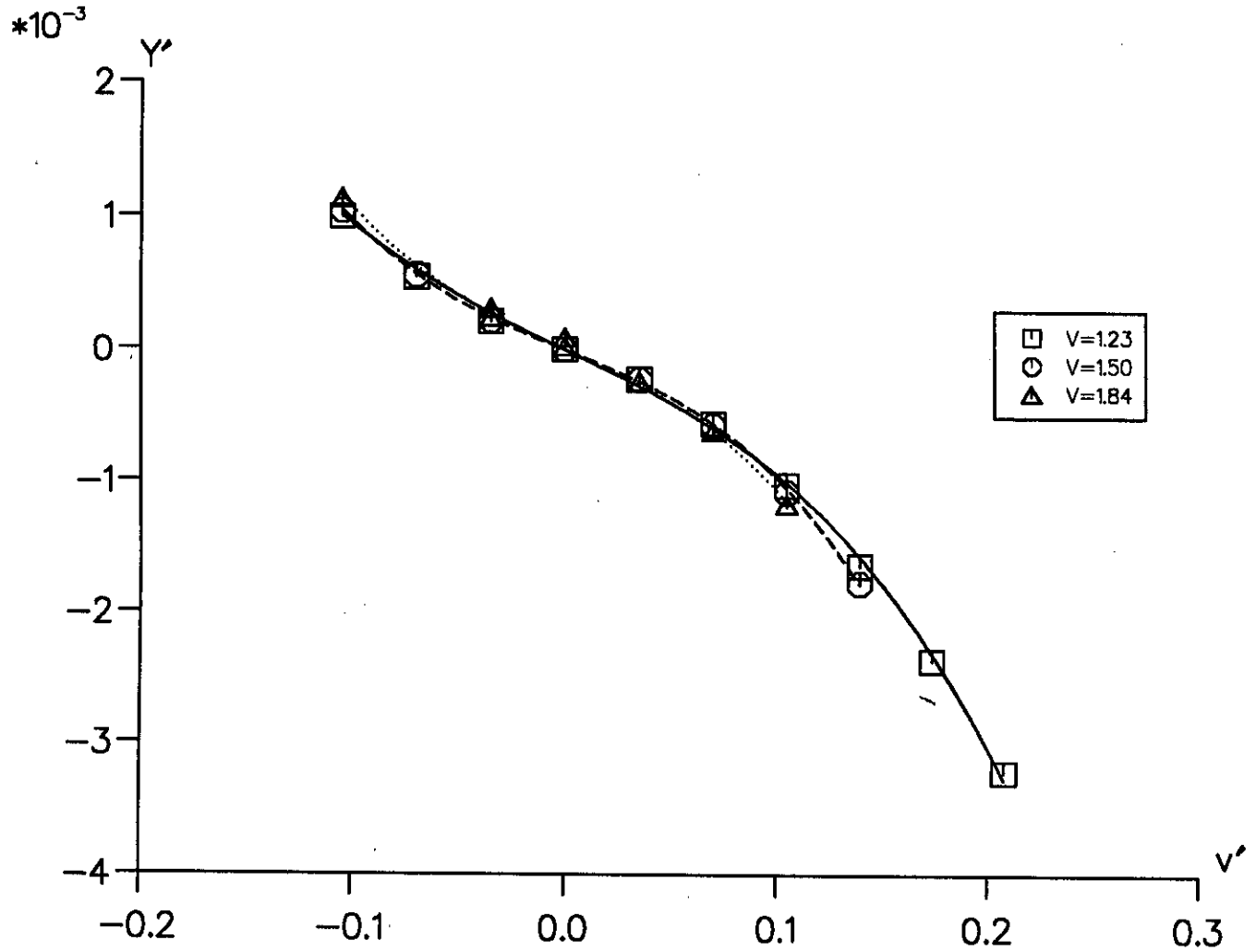

Fig.4 Leander Static Test N′ vs. v′

Fwd LCG

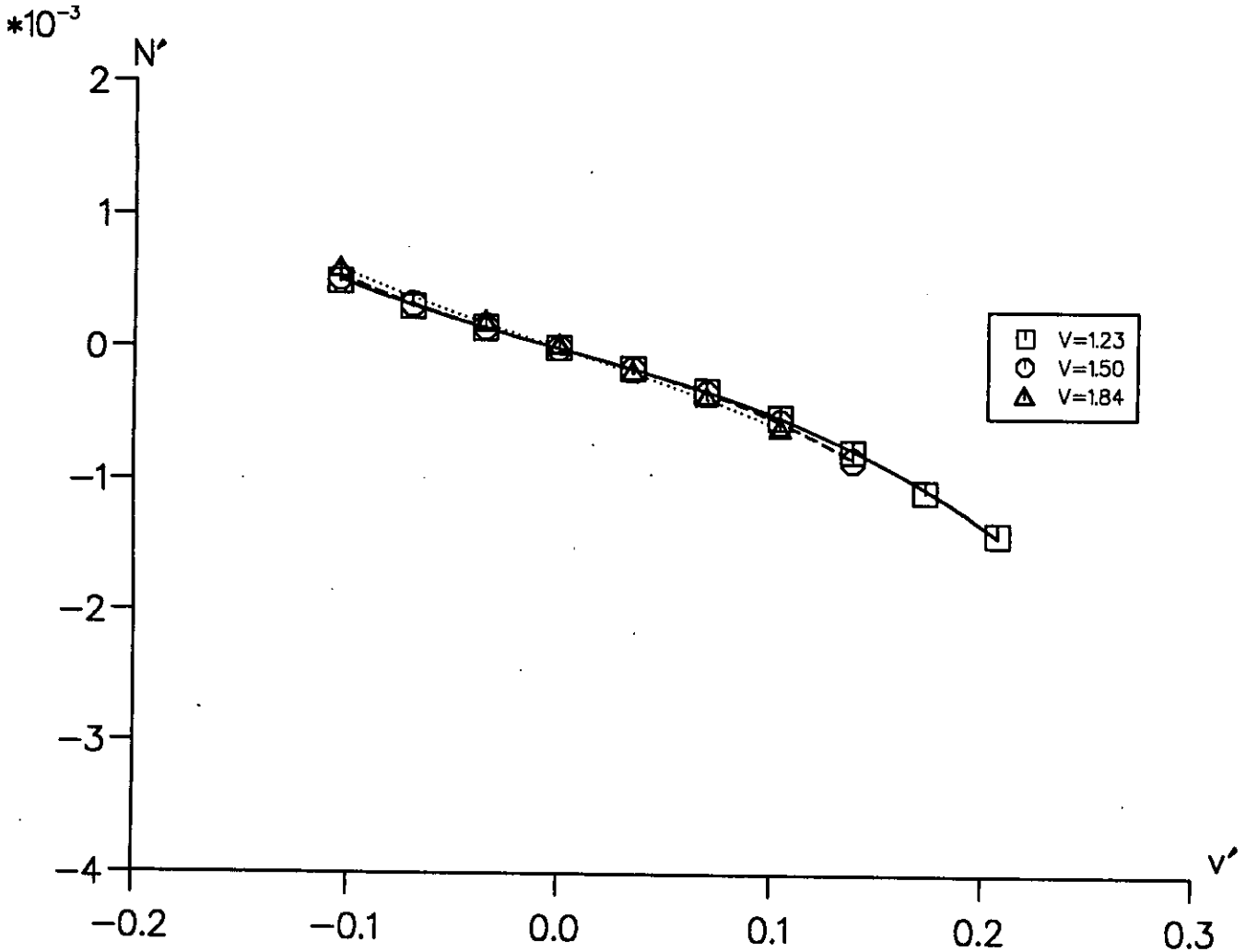

Fig.5 Leander Sway Test Y1quad vs. v'

V = 1.23 m/s

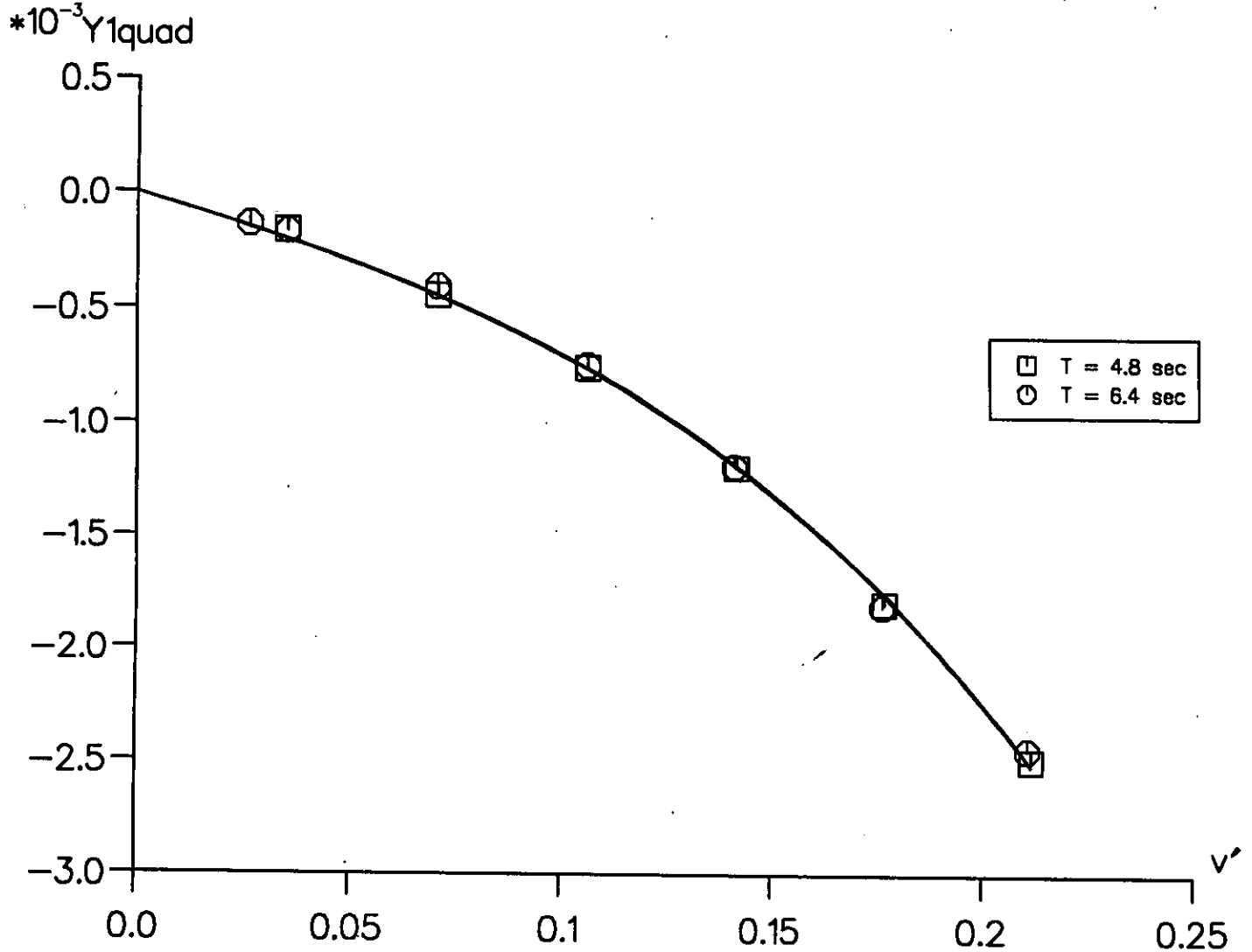

Fig.6 Leander Sway Test N1quad vs. v'

V = 1.23 m/s

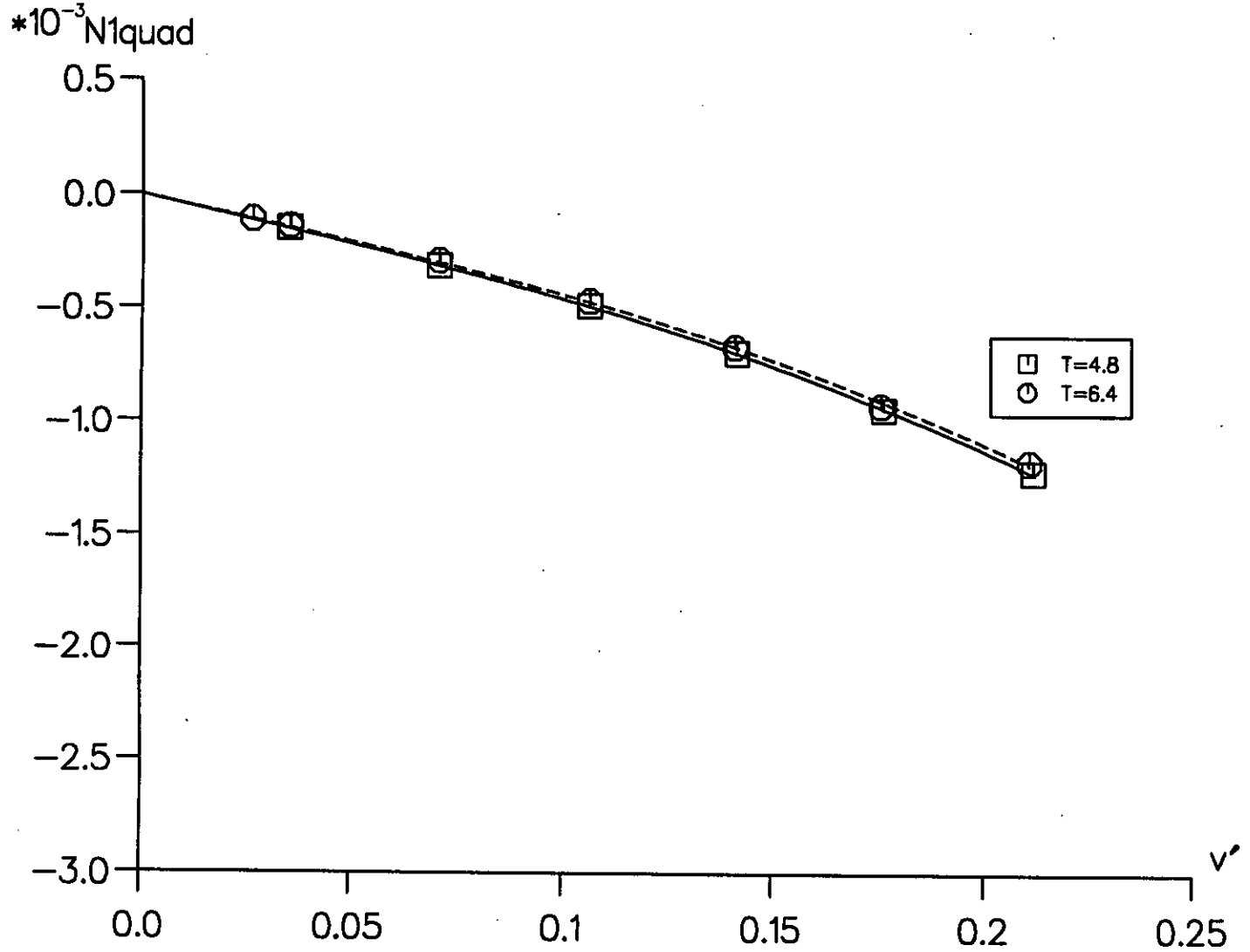

Fig.7 Leander Sway Test Y1in vs. Vdot

V = 1.23 m/s

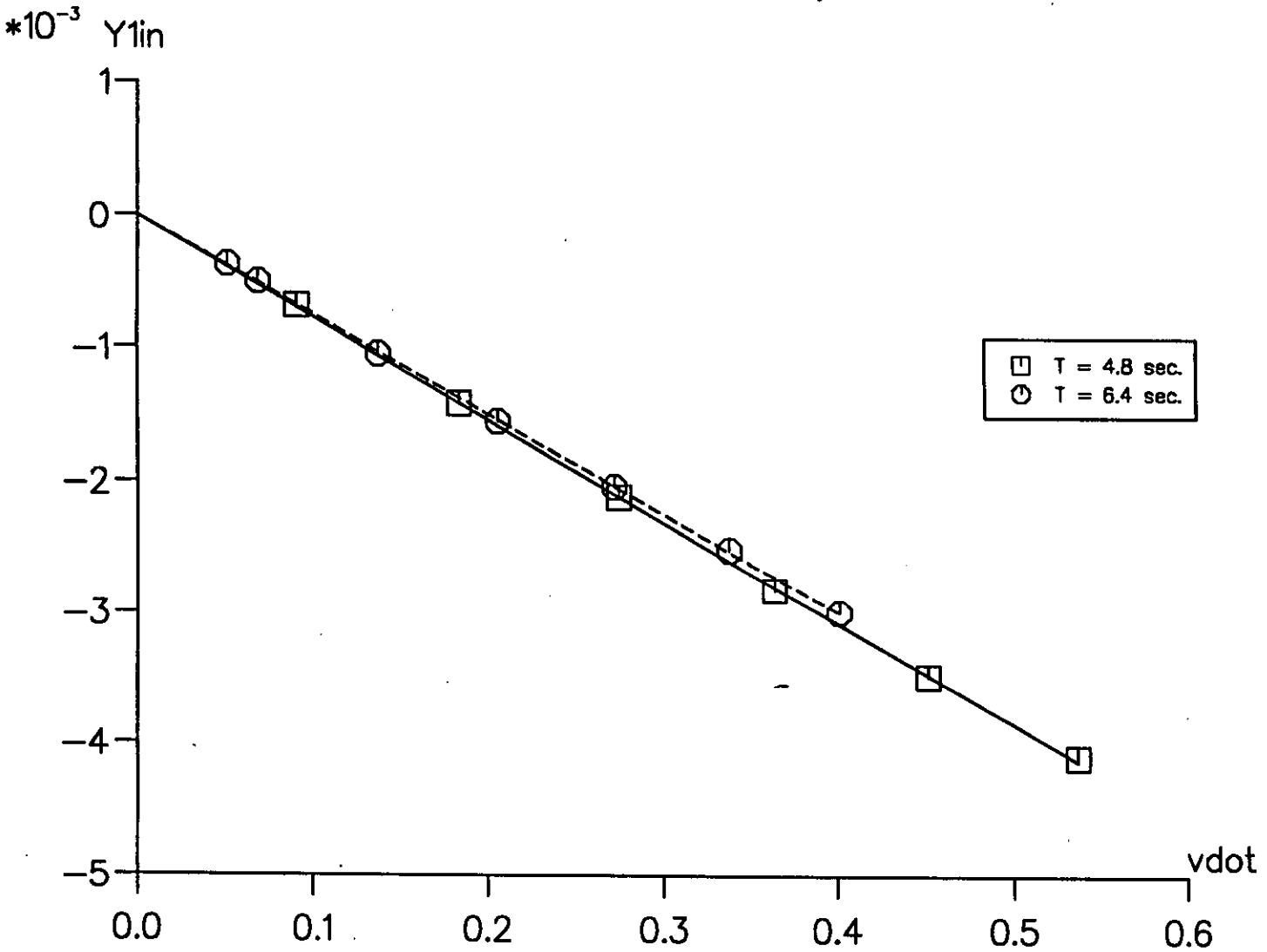

Fig.8 Leander Sway Test N1in vs. vdot

V = 1.23

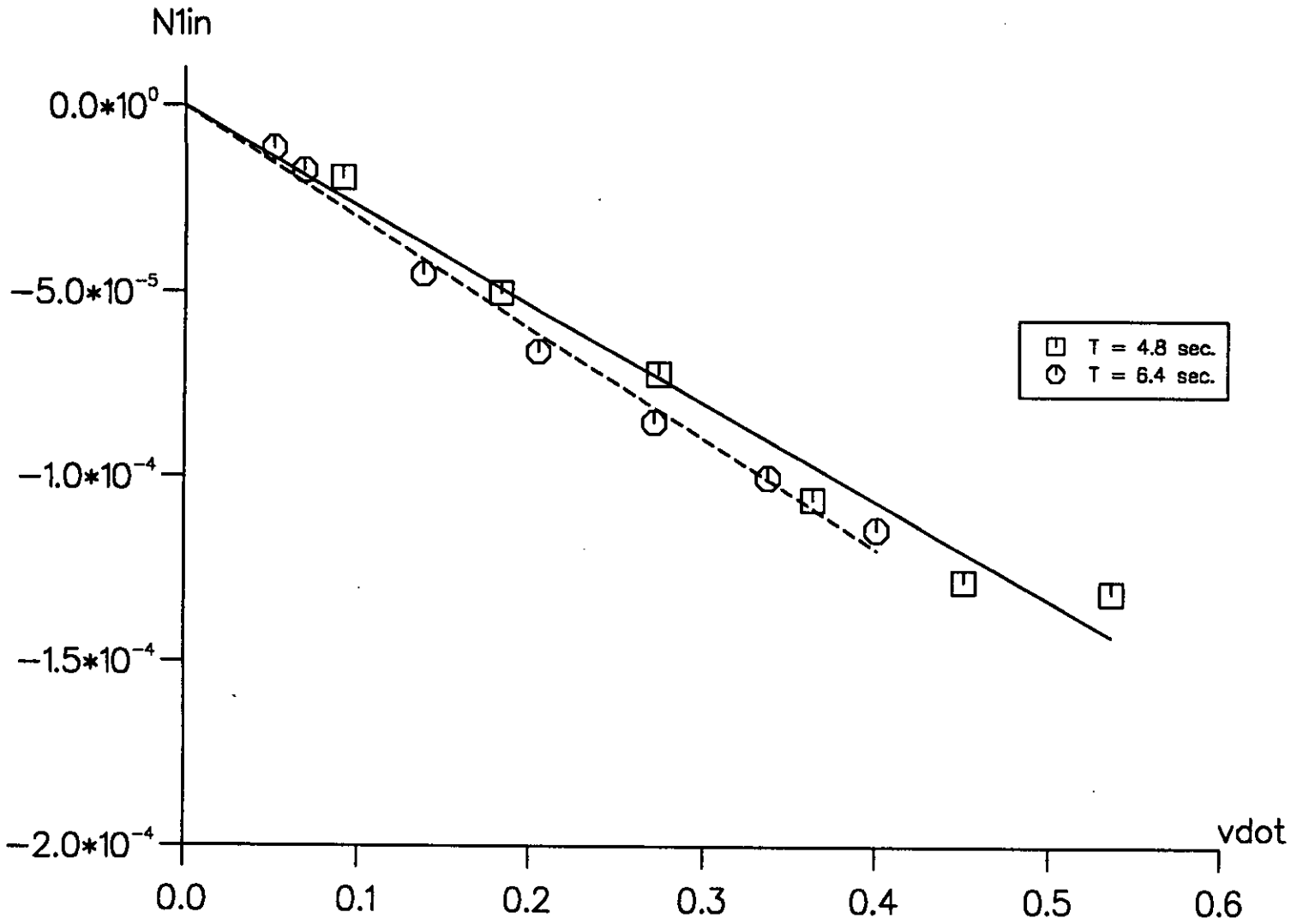

Fig.9 Leander Sway Test Y1quad vs. v'

V = 1.50 m/s

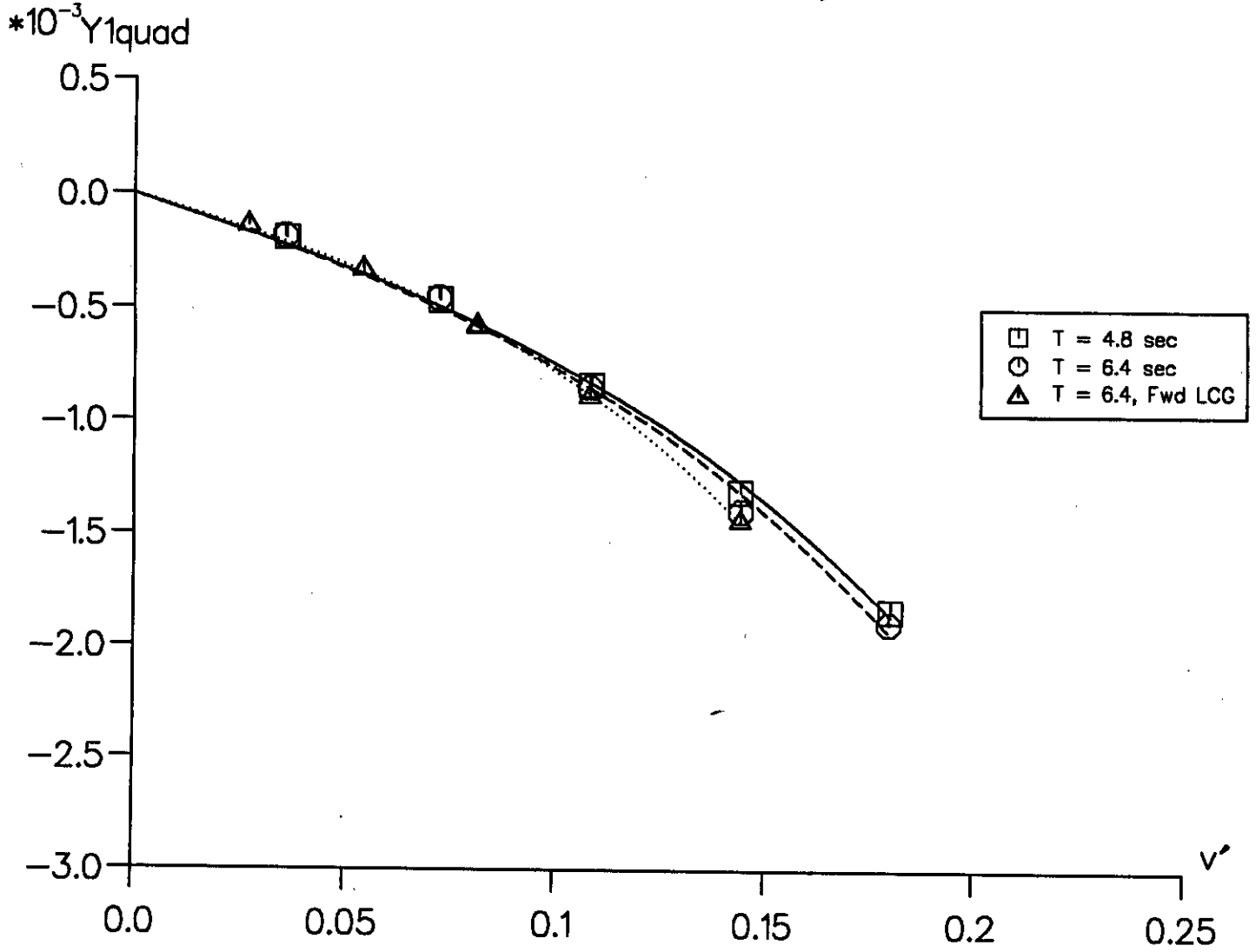

Fig.10 Leander Sway Test N1quad vs. v'

V = 1.50 m/s

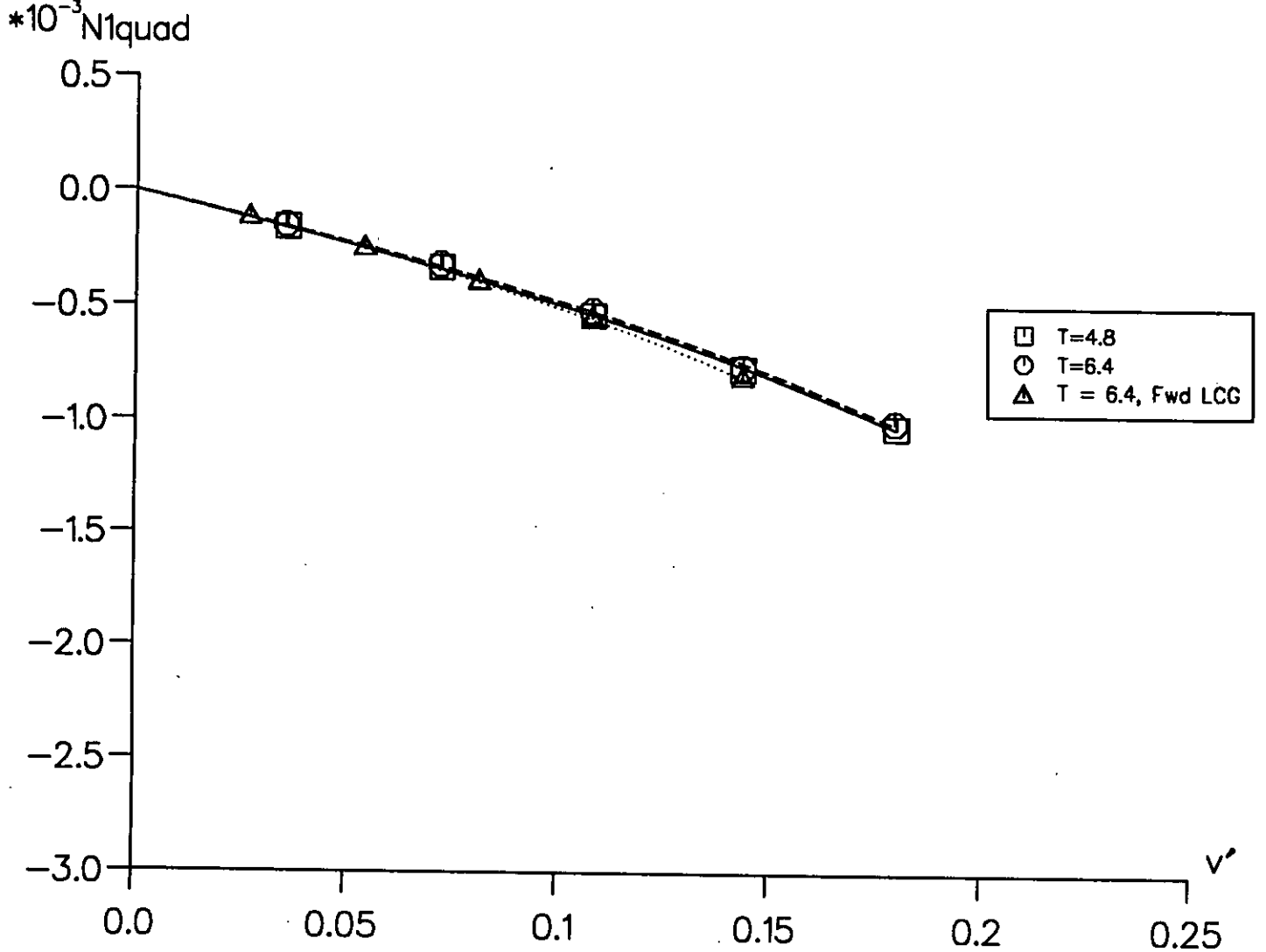

Fig.11 Leander Sway Test Y1in vs. Vdot

V = 1.50 m/s

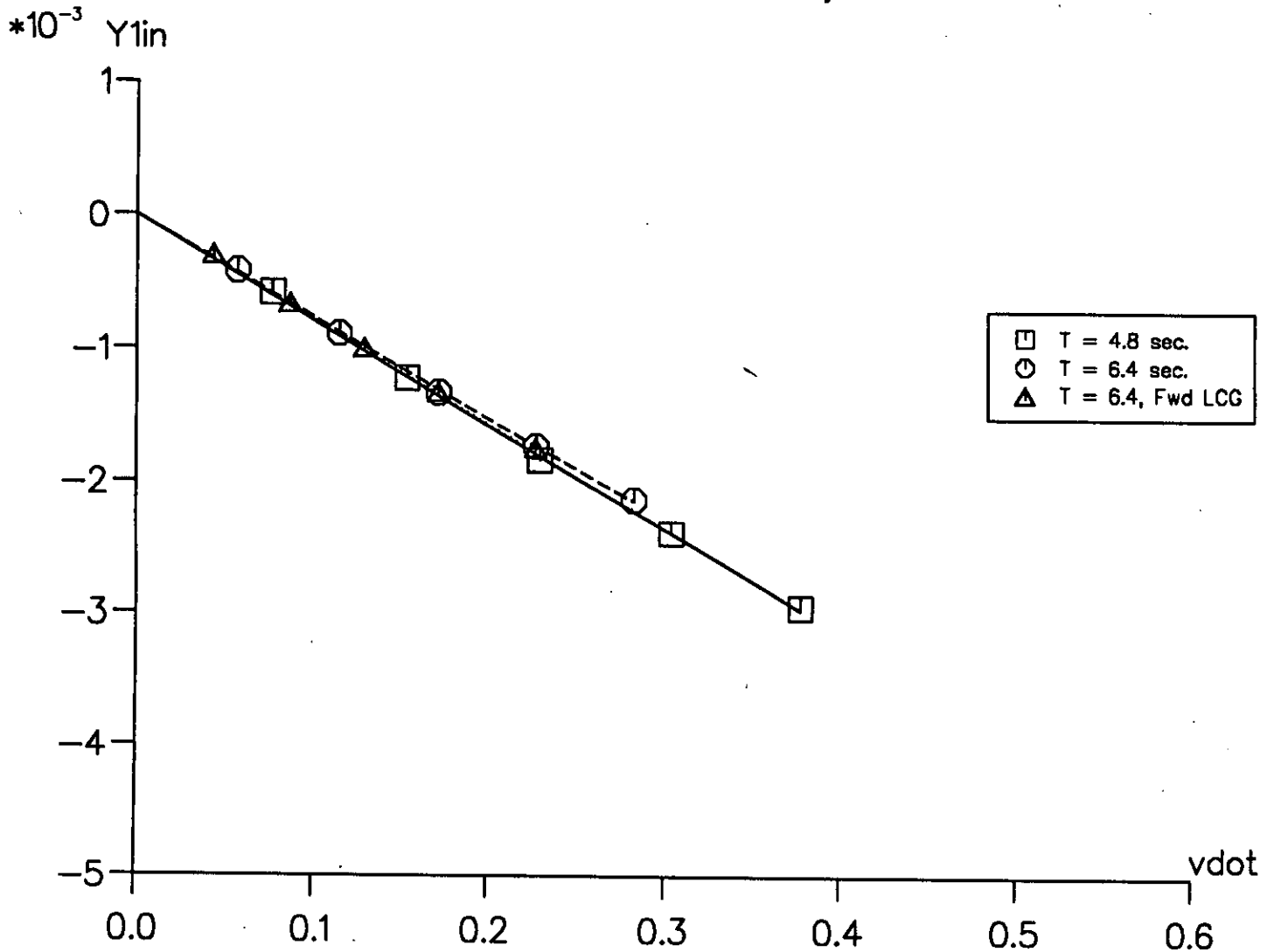

Fig.12 Leander Sway Test N1in vs. vdot

V = 1.50 m/s

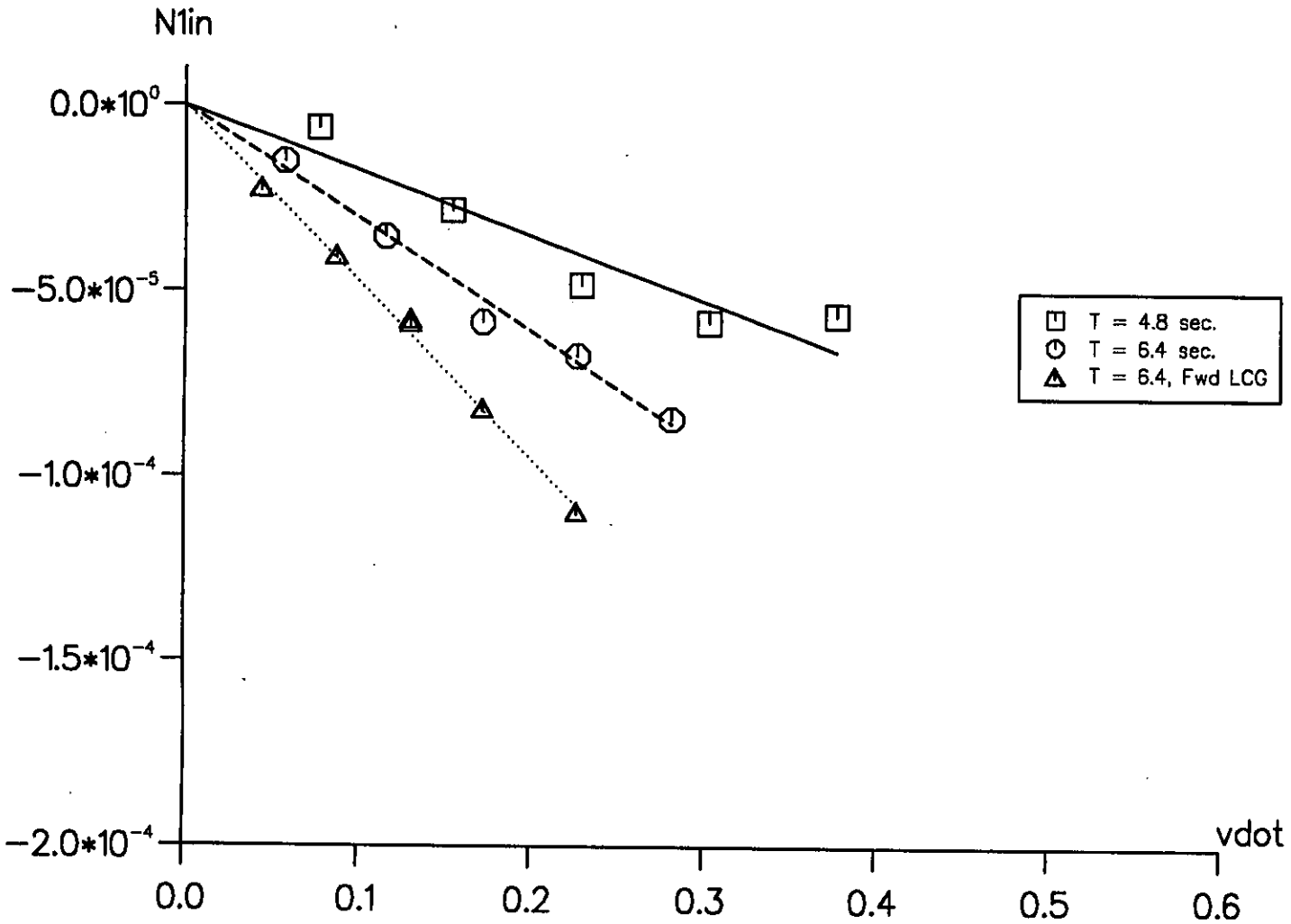

Fig.13 Leander Sway Test Y1quad vs. v'

V = 1.84 m/s

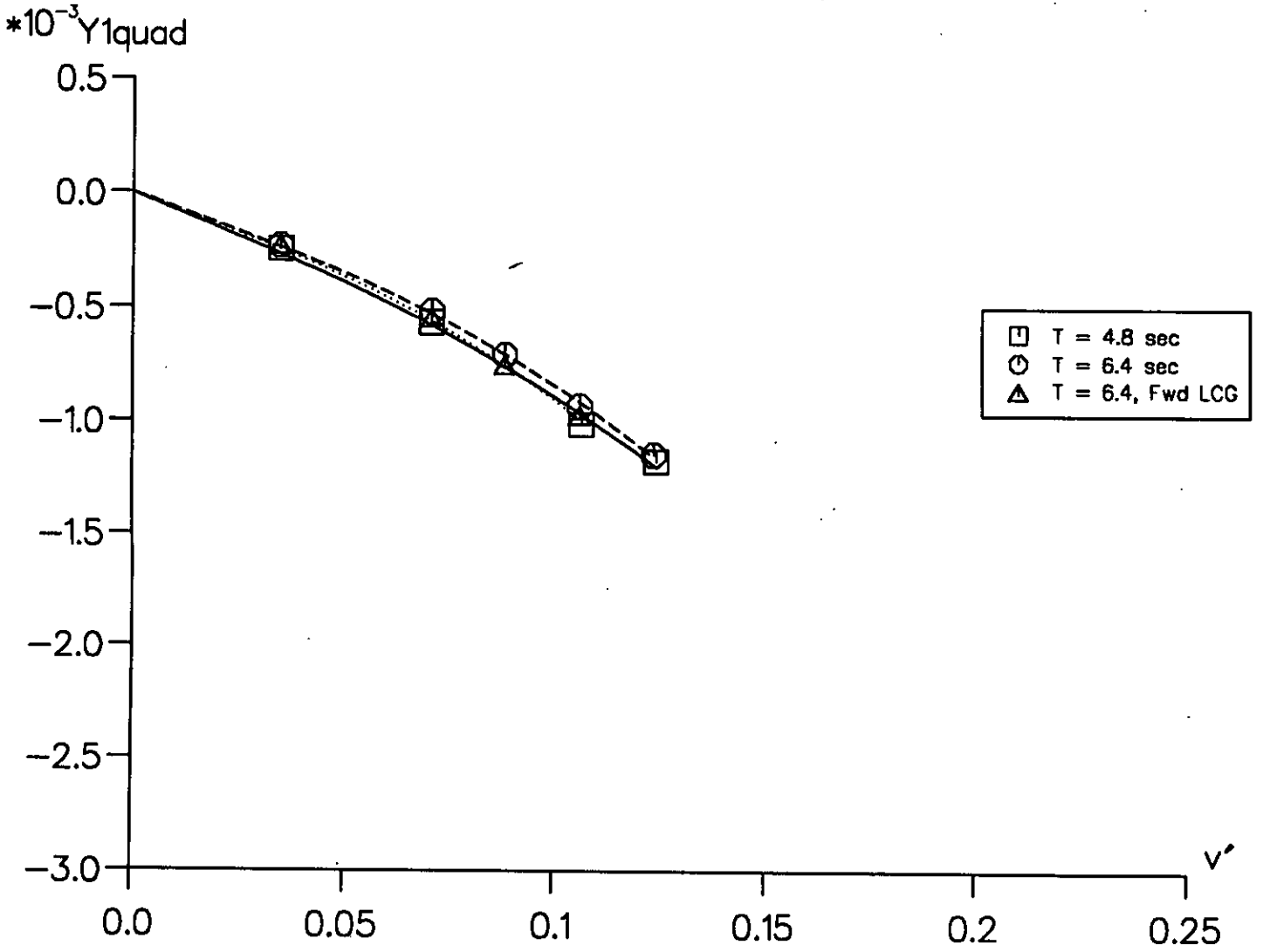

Fig.14 Leander Sway Test N1quad vs. v'

V = 1.84 m/s

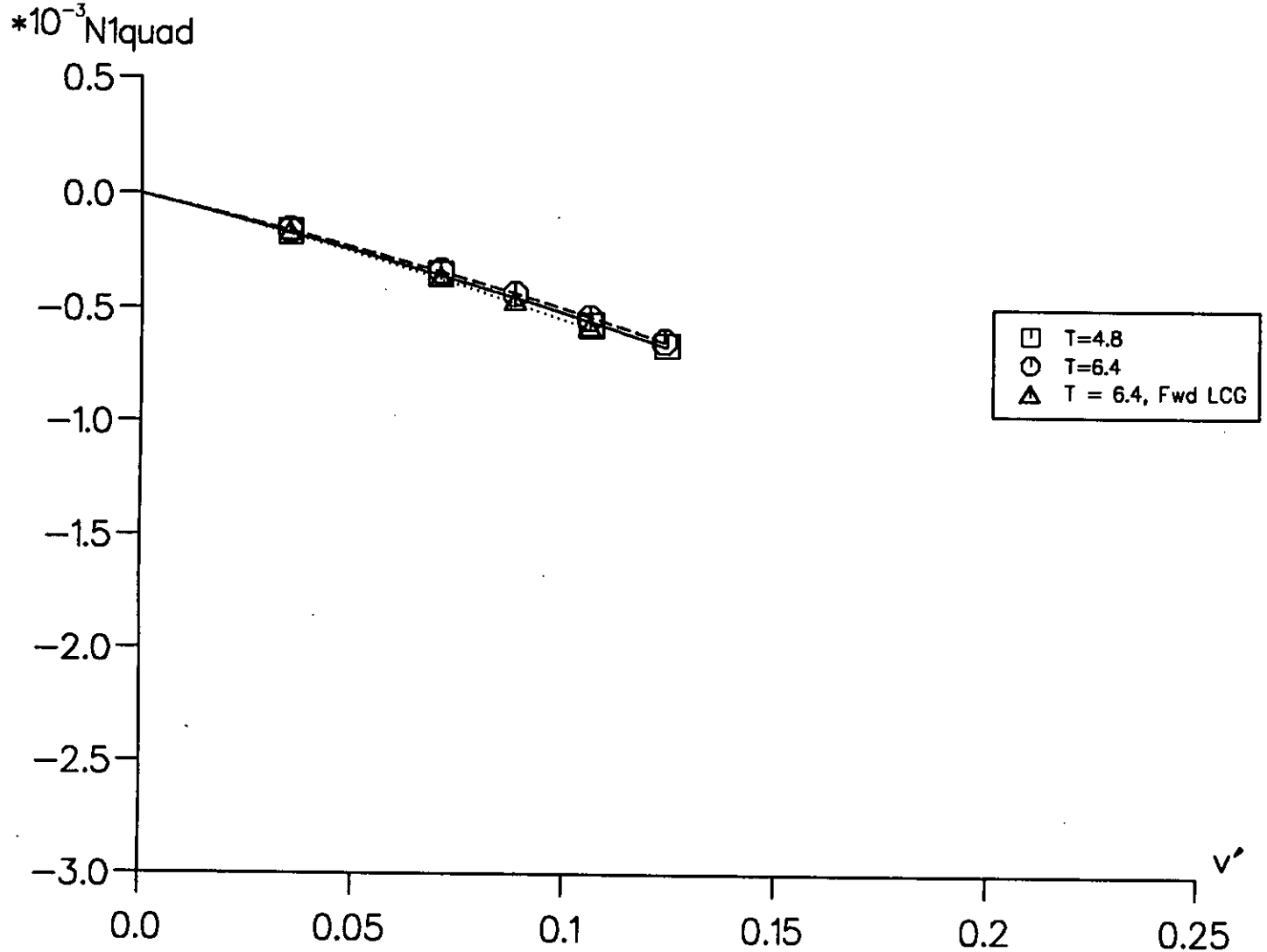

Fig.15 Leander Sway Test Y1in vs. Vdot

V = 1.84 m/s

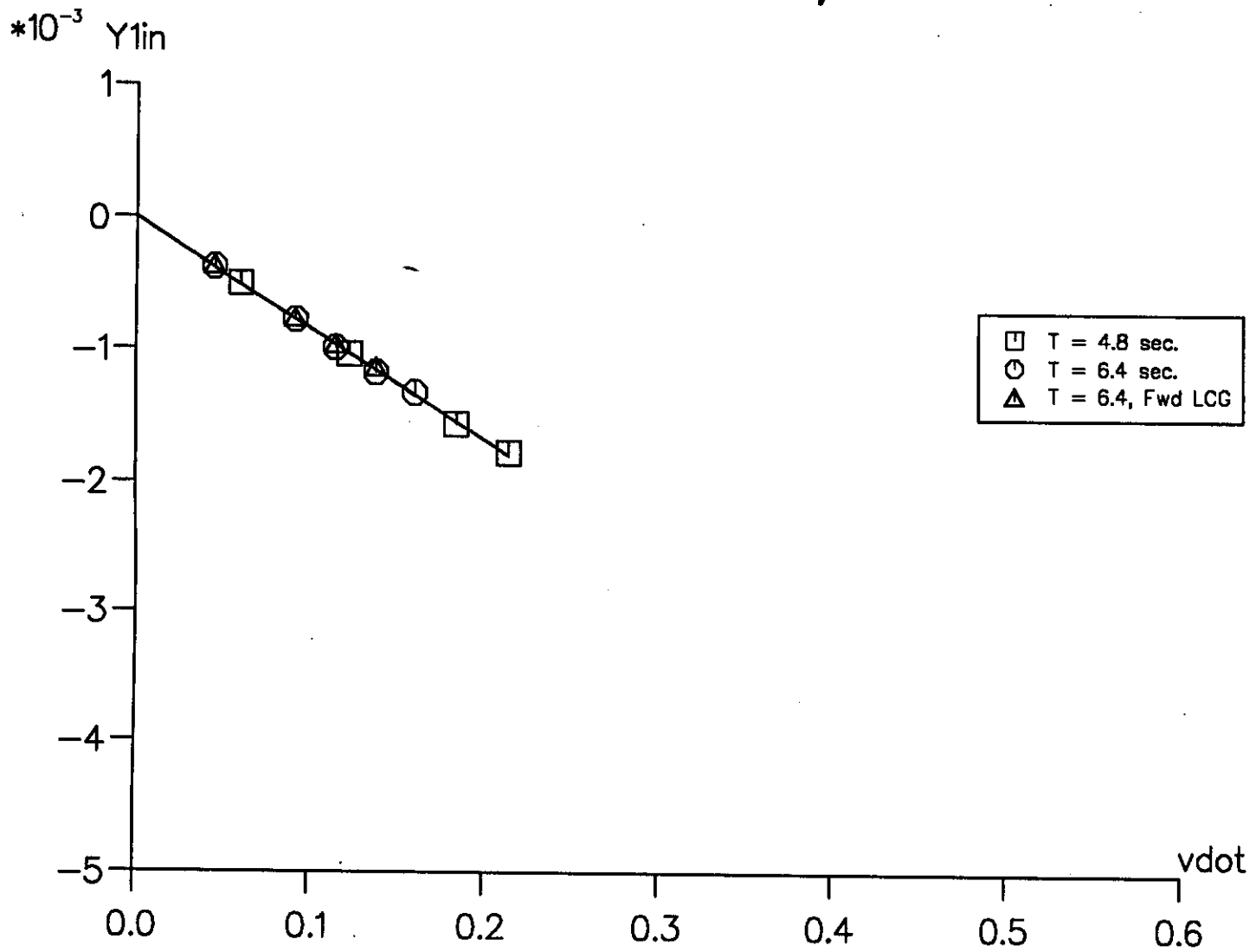

Fig.16 Leander Sway Test N1in vs. vdot

V = 1.84 m/s

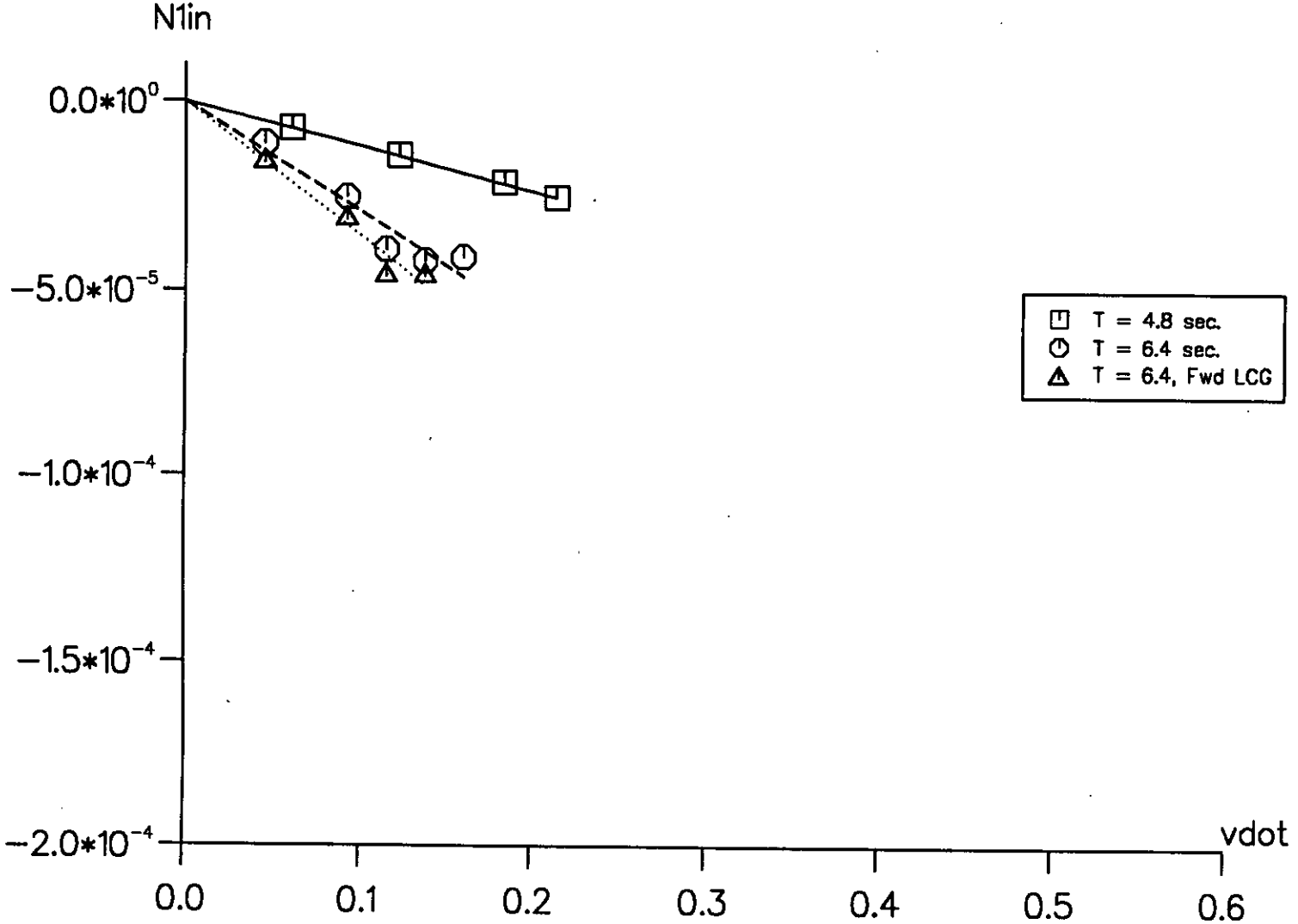

Fig.17 Leander Yaw Test Y1quad vs. r'

V = 1.23 m/s

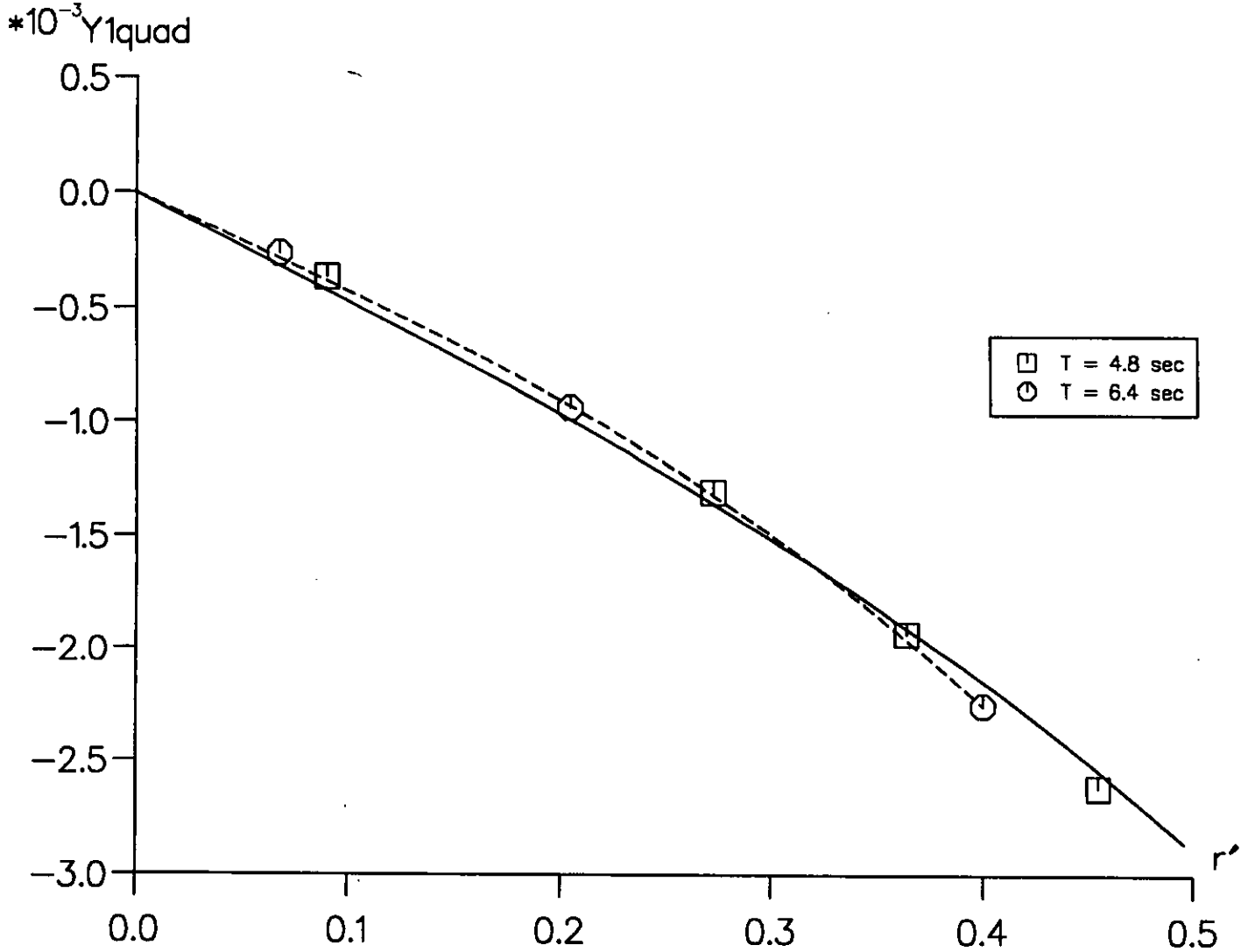

Fig.18 Leander Yaw Test N1quad vs. r′

V = 1.23 m/s

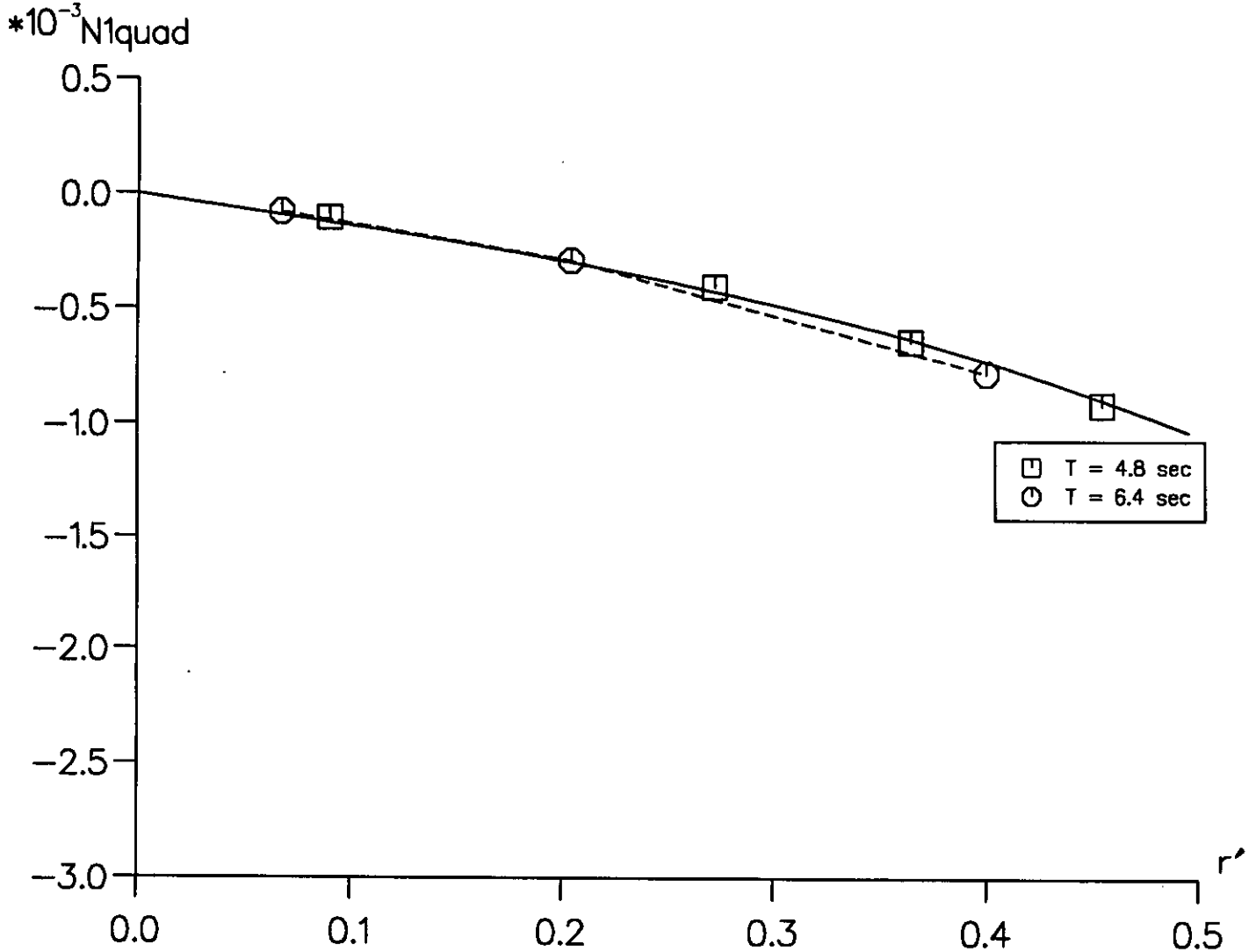

Fig.19 Leander Yaw Test Y1in vs. rdot

V = 1.23 m/s

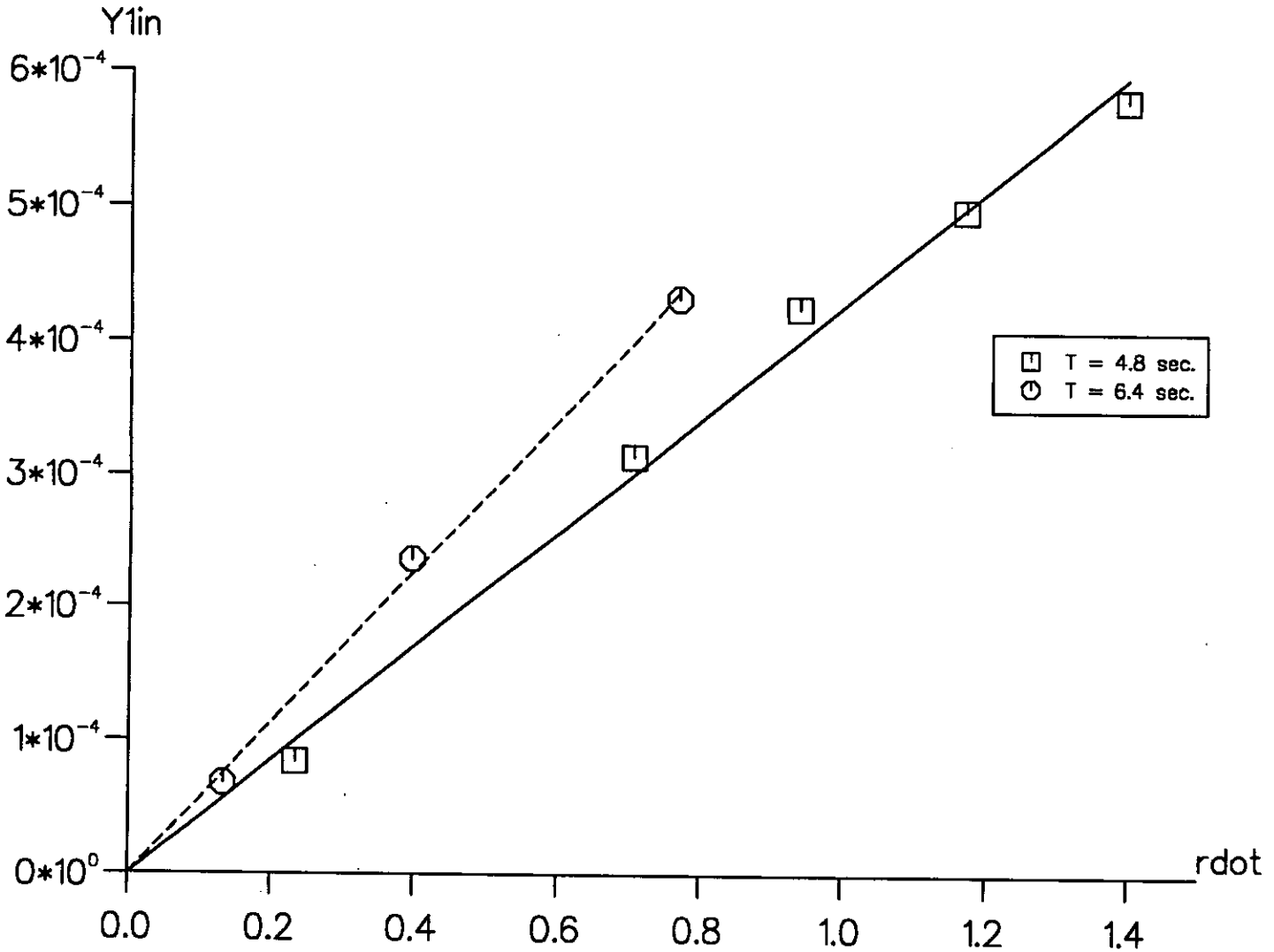

Fig.20 Leander Yaw Test N1in vs. rdot

V = 1.23 m/s

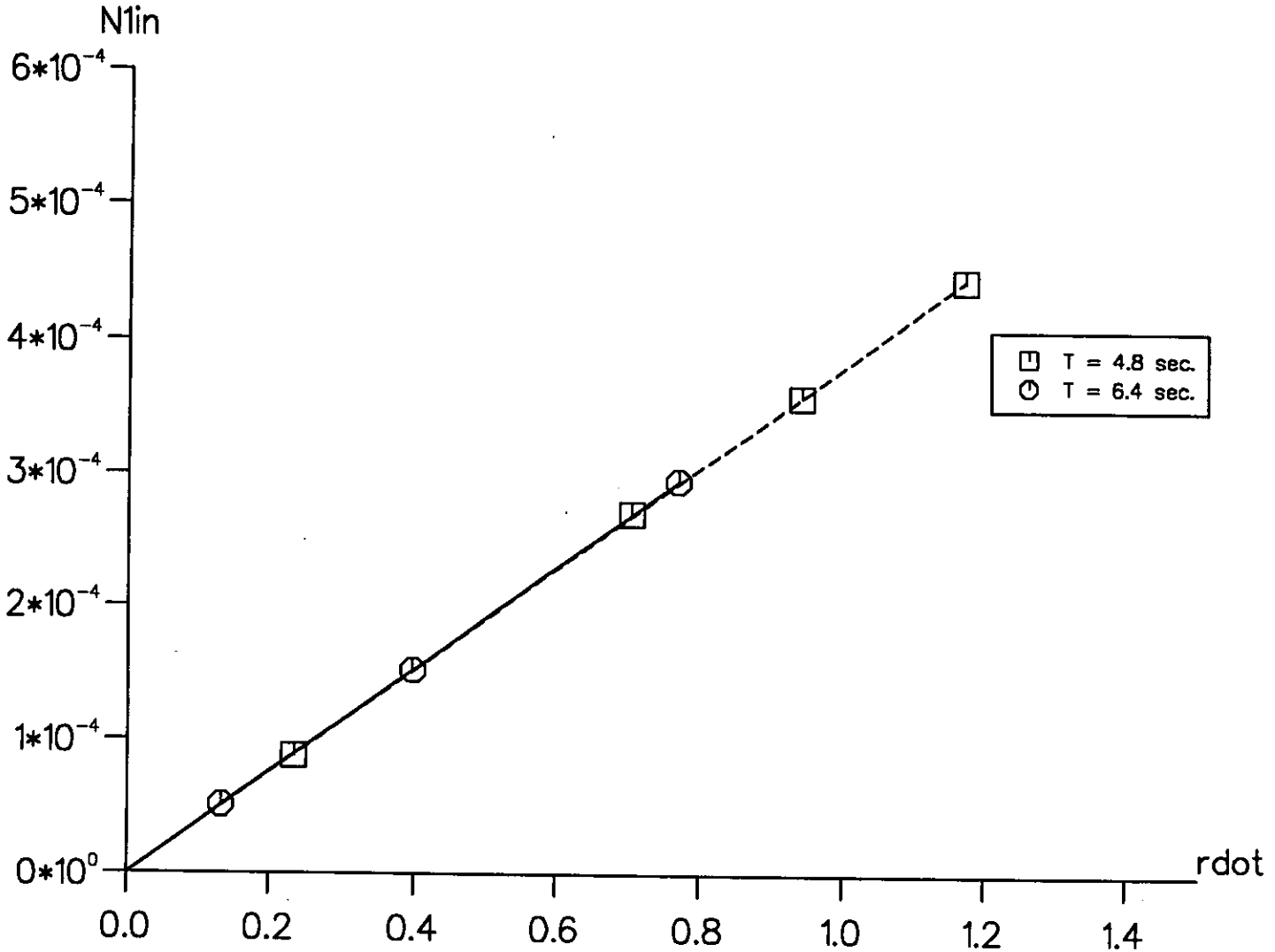

Fig.21 Leander Yaw Test Y1quad vs. r'

V = 1.50 m/s

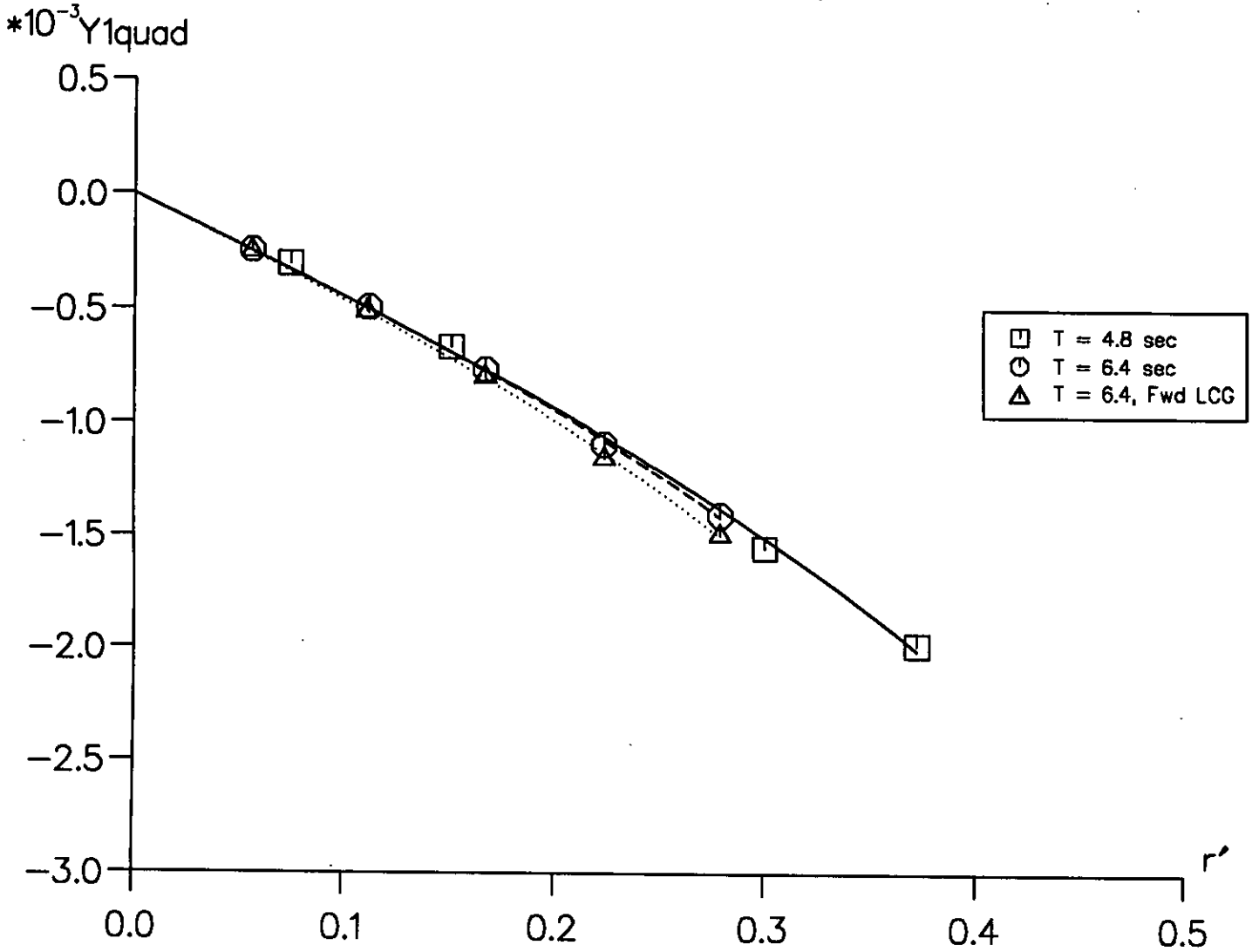

Fig.22 Leander Yaw Test N1quad vs. r′

V = 1.50 m/s

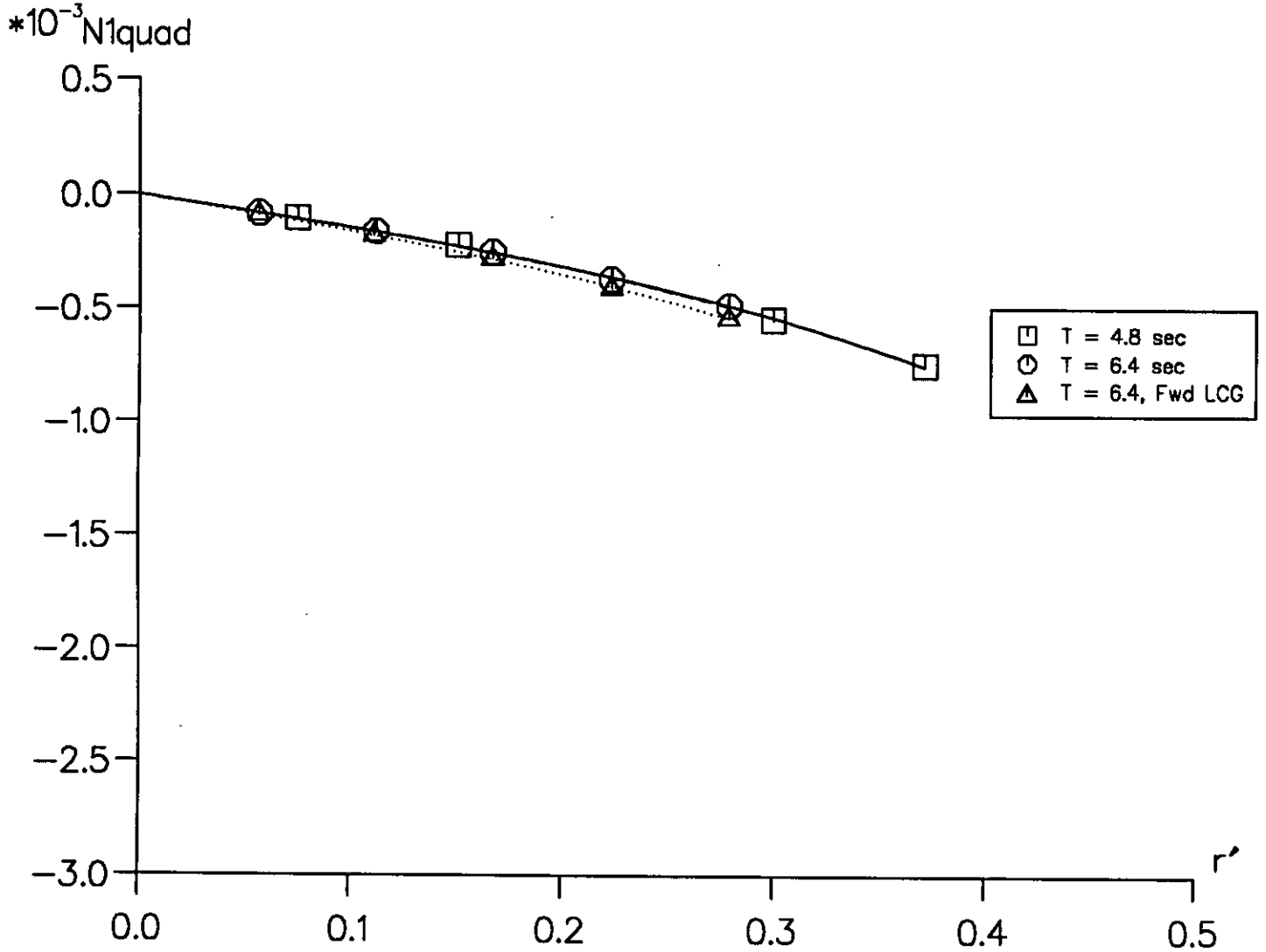

Fig.23 Leander Yaw Test Y1in vs. rdot

V = 1.50 m/s

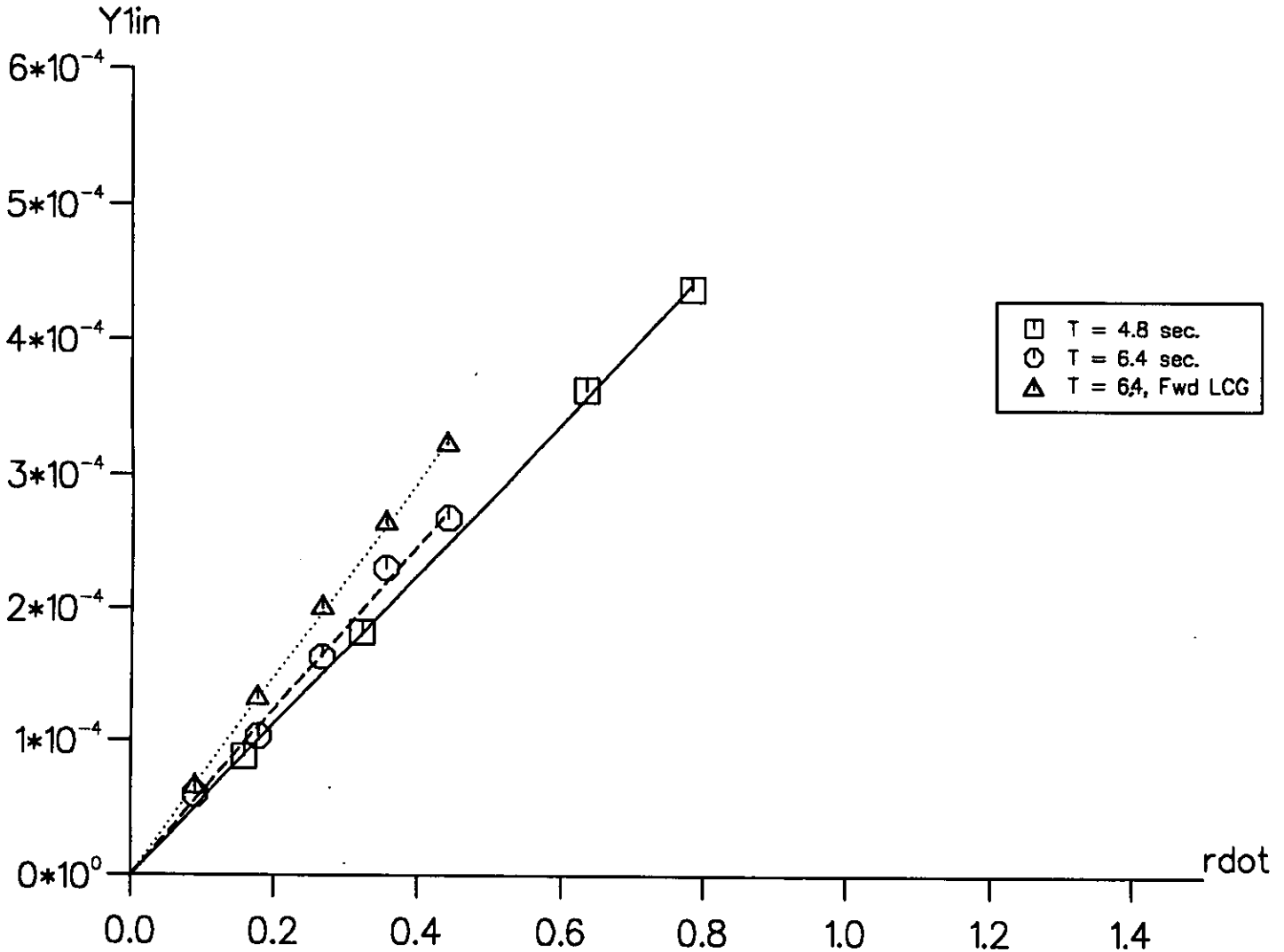

Fig.24 Leander Yaw Test N1in vs. rdot

V = 1.50 m/s

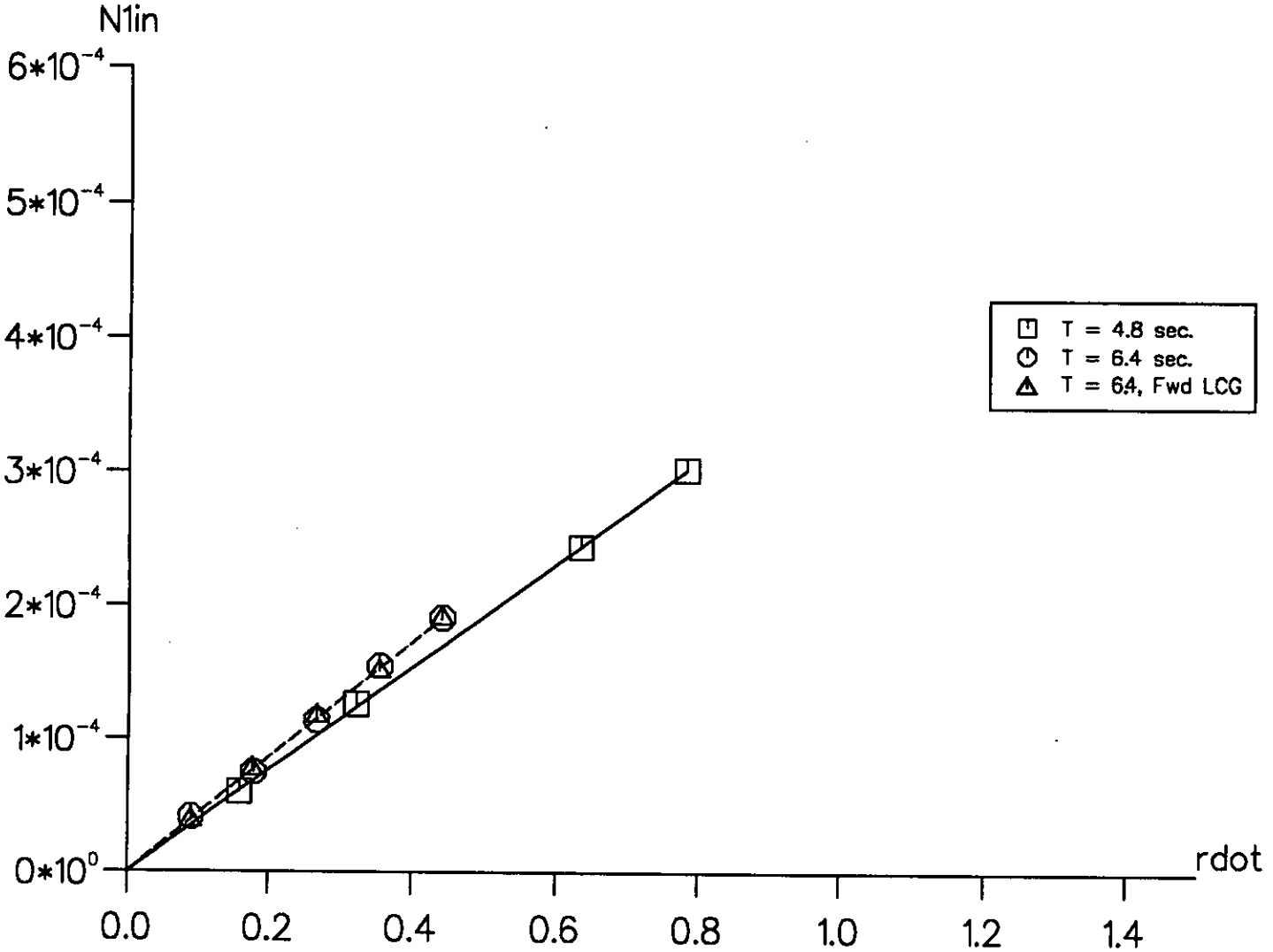

Fig.25 Leander Yaw Test Y1quad vs. r′

V = 1.84 m/s

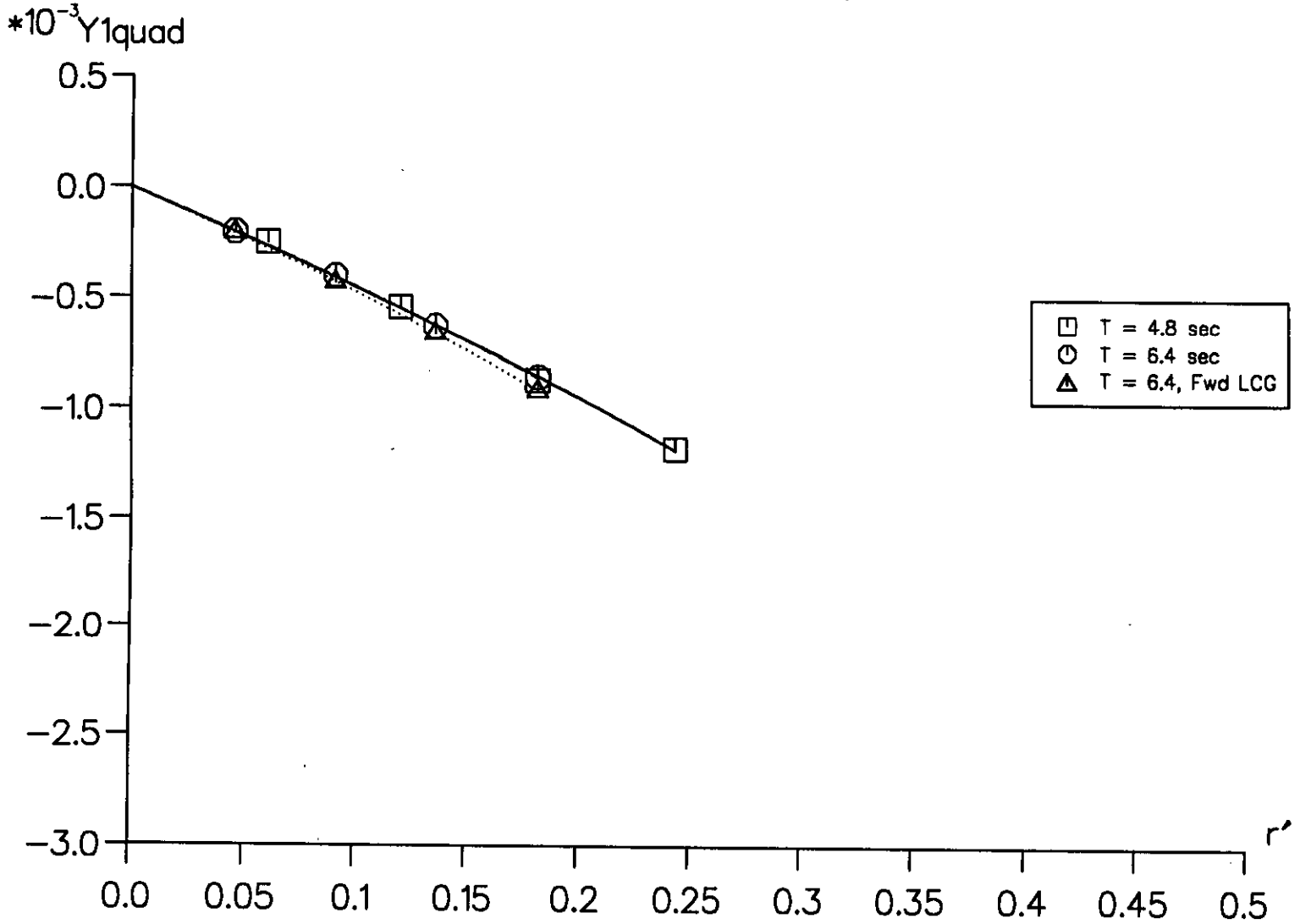

Fig.26 Leander Yaw Test N1quad vs. r′

V = 1.84 m/s

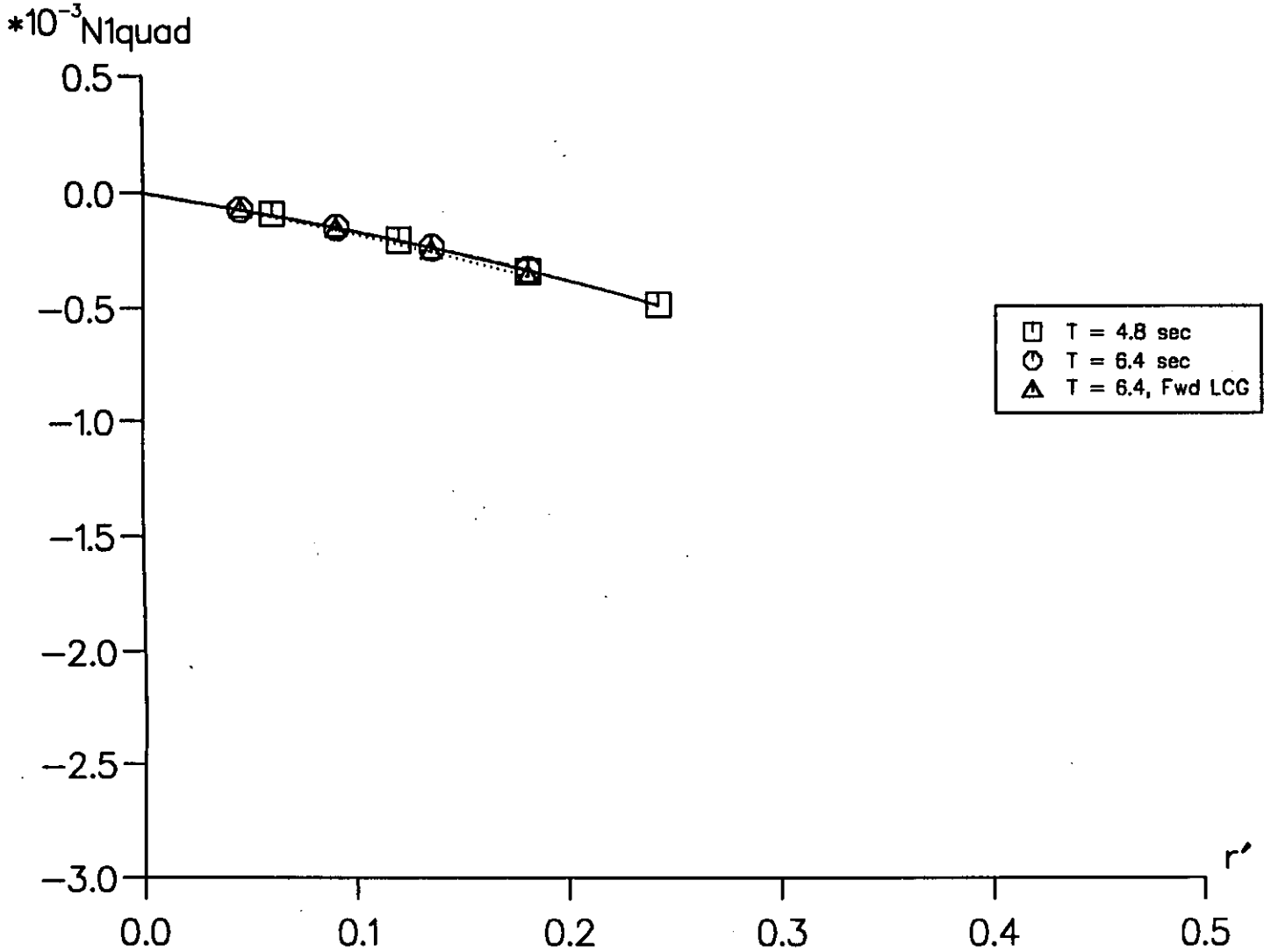

Fig.27 Leander Yaw Test Y1in vs. rdot

V = 1.84 m/s

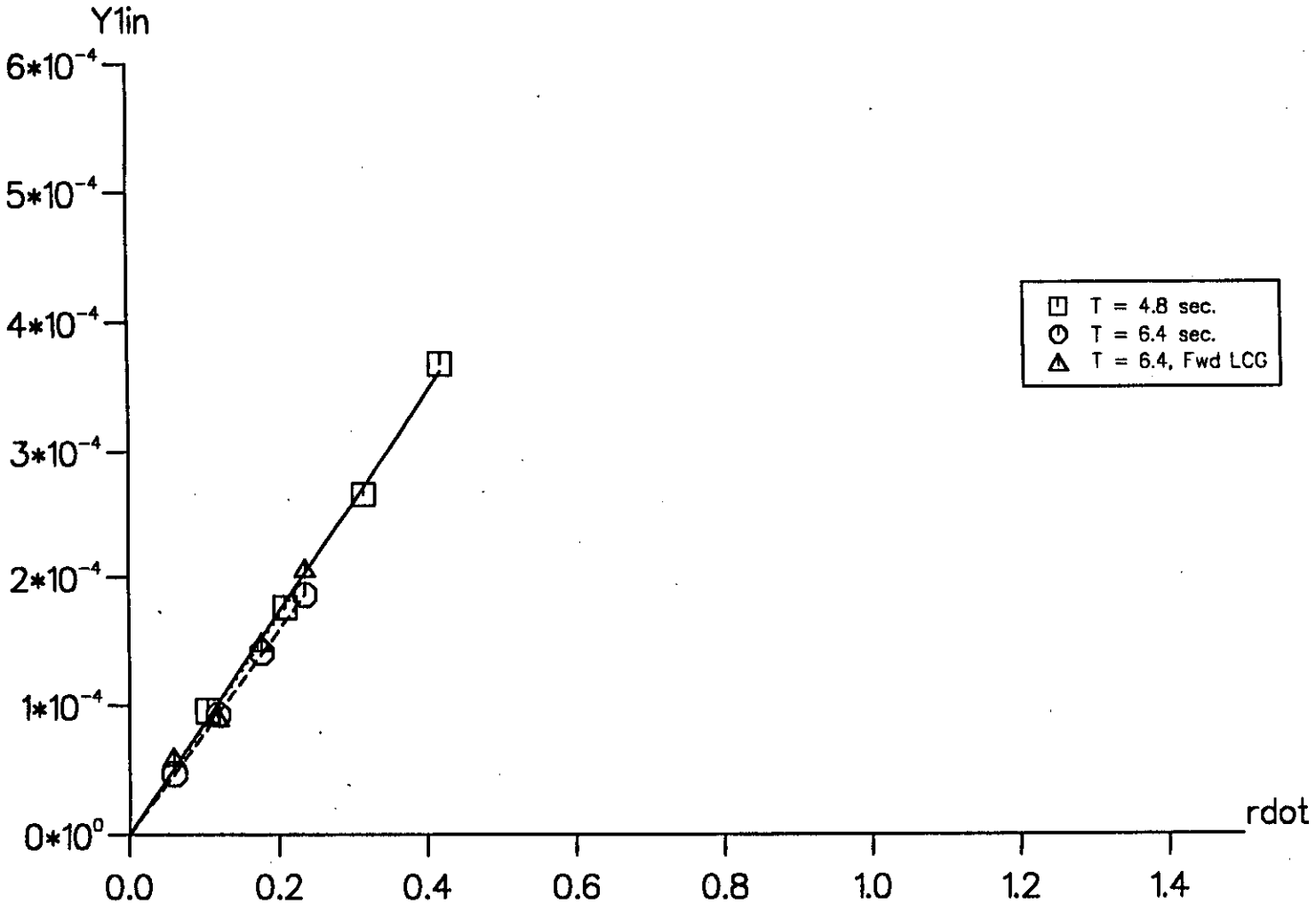

Fig.28 Leander Yaw Test N1in vs. rdot

V = 1.84 m/s

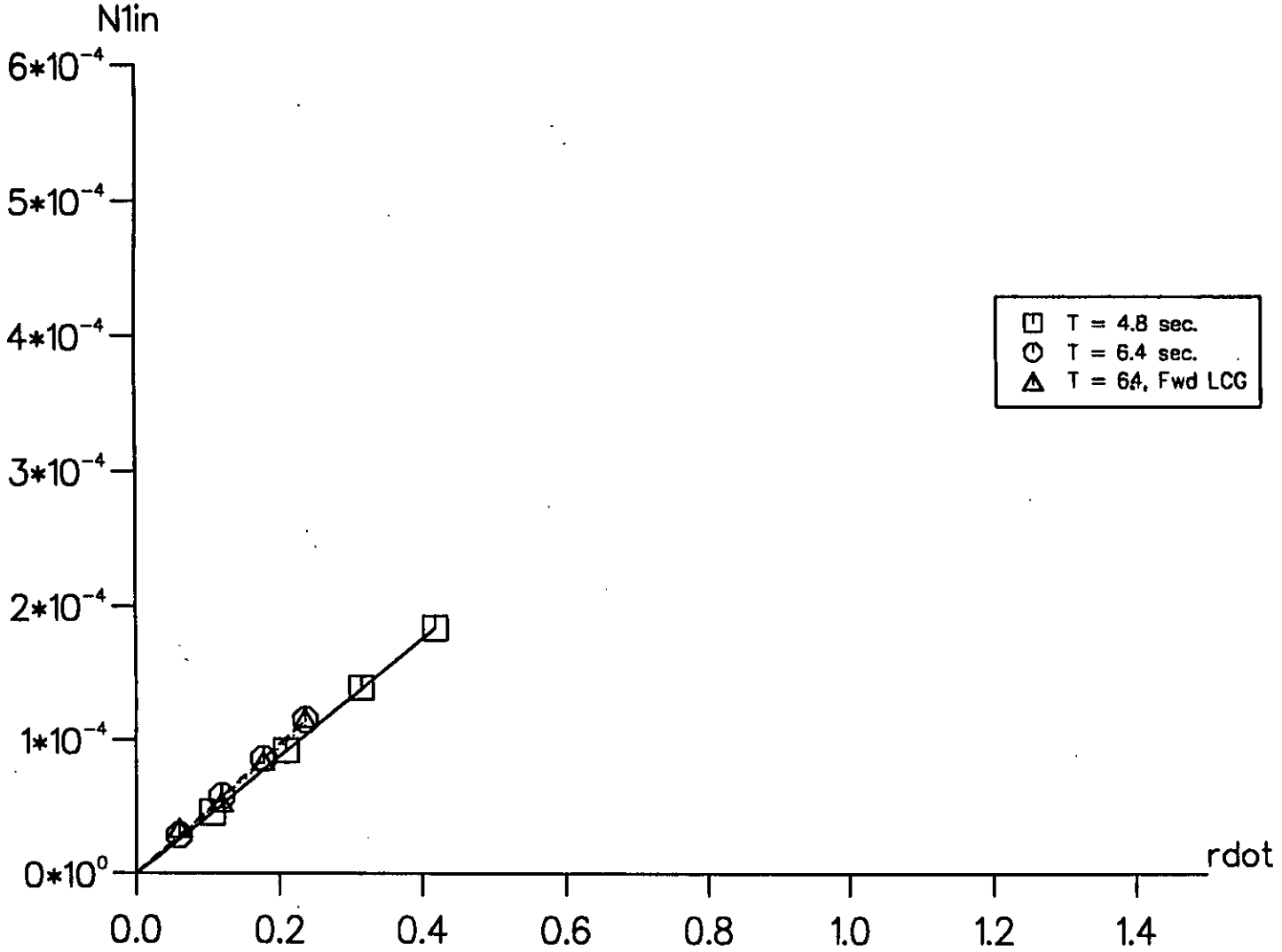

Fig.29 The Leander Hull

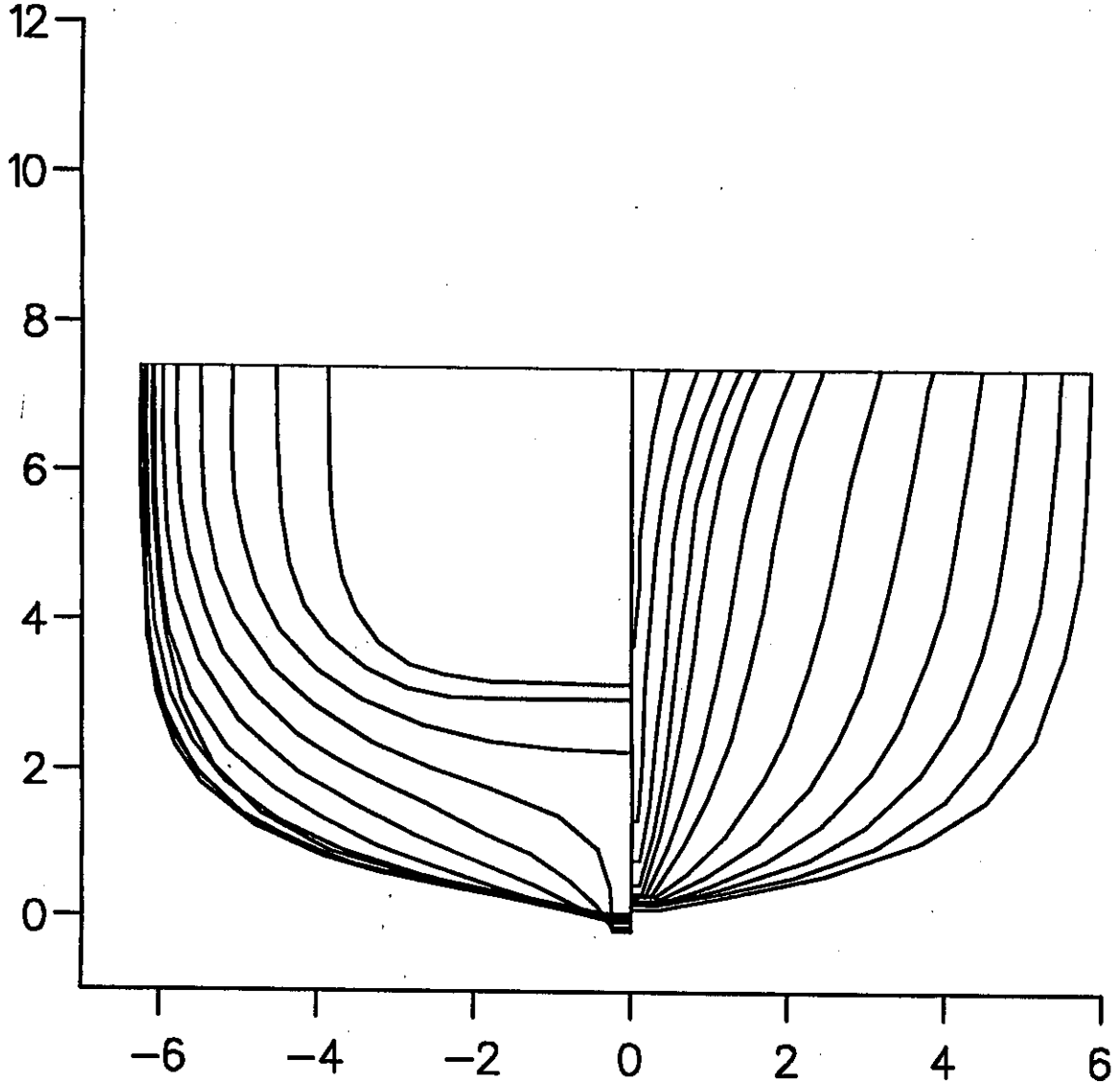

Stern

Bow

Fig.30 A Side-view of the Streamlines on the "Leander" Hull

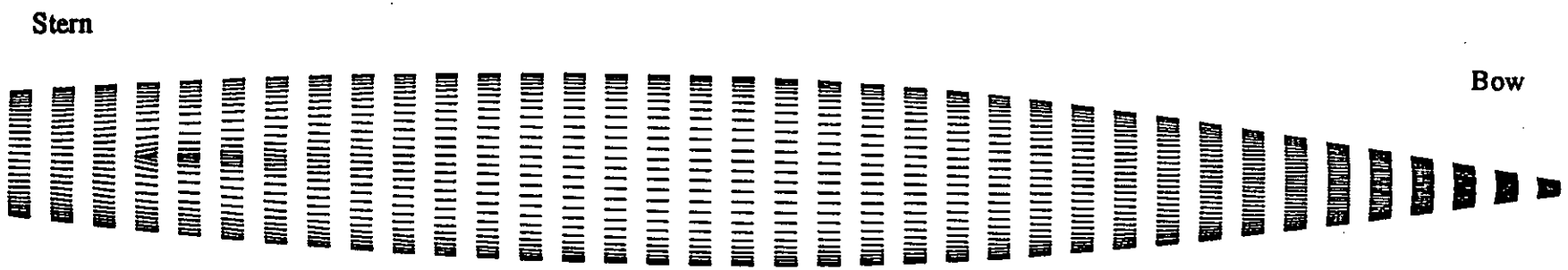


Fig.31 A Bottom-view of the Streamlines on the "Leander" Hull

Fig.32 Comparison of Calculated Sway Force with PMM Test for the Leander Hull

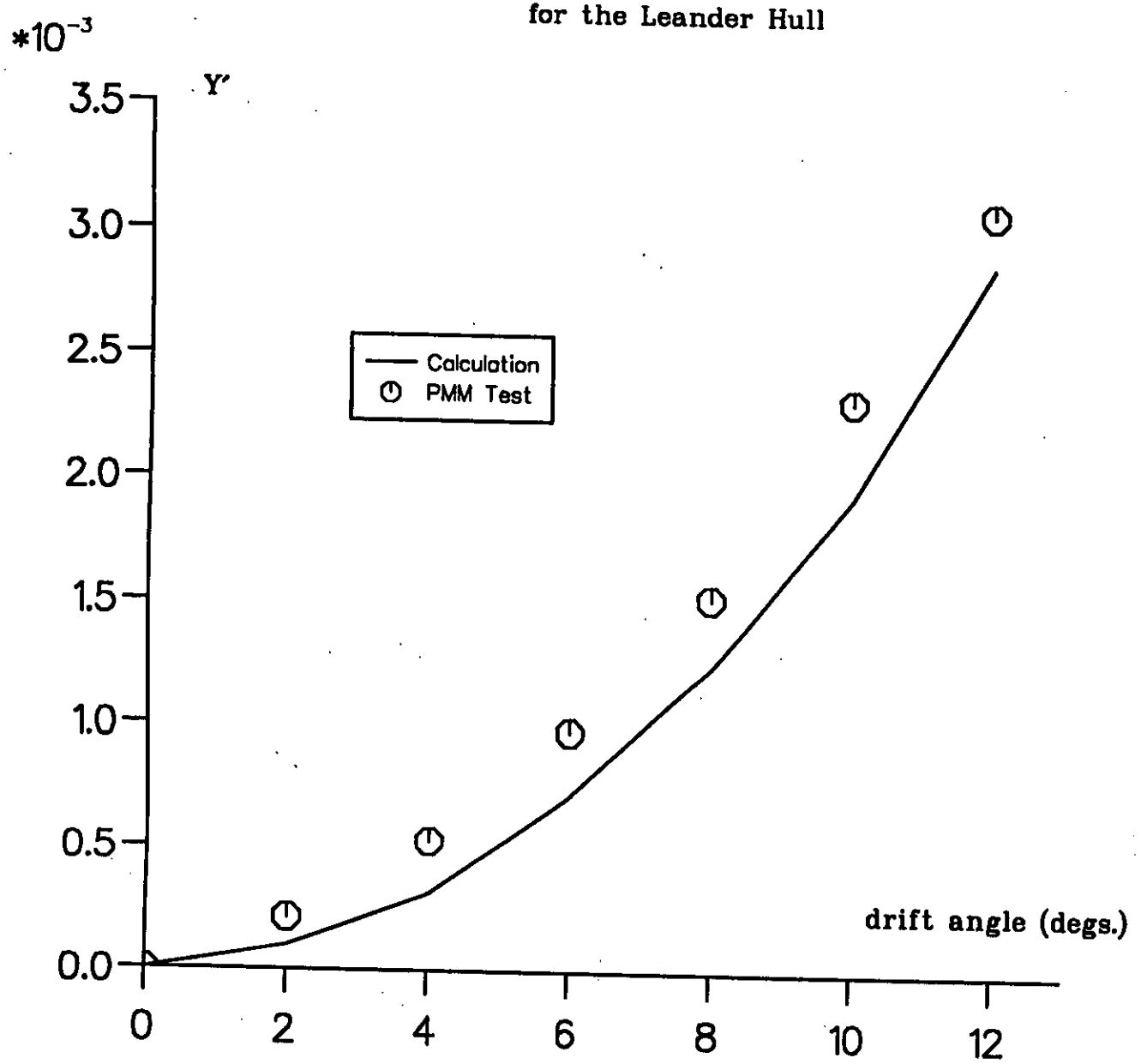

Fig.33 Comparison of Calculated Yaw Moment with PMM Test for the Leander Hull

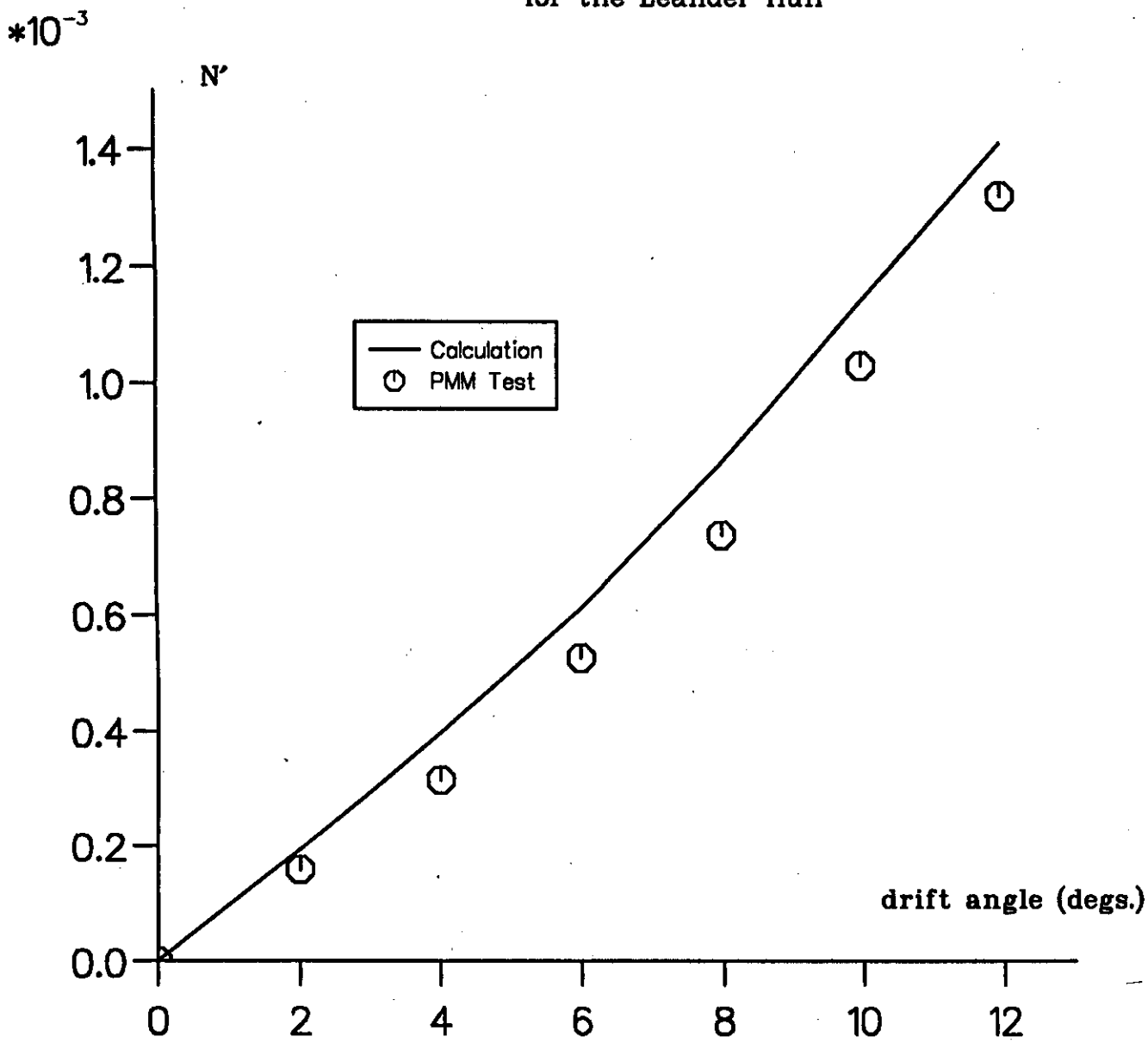

Fig.34 Side Force Distribution on the Leander Hull